

A TESS DRESS REHEARSAL: PLANETARY CANDIDATES AND VARIABLES FROM K2 CAMPAIGN 17

IAN J. M. CROSSFIELD¹, NATALIA GUERRERO¹, TREVOR DAVID², SAMUEL N. QUINN³, ADINA D. FEINSTEIN⁴, CHELSEA HUANG¹, LIANG YU¹, KAREN A. COLLINS³, BENJAMIN J. FULTON⁵, BJÖRN BENNEKE⁶, MERRIN PETERSON⁶, ALLYSON BIERYLA³, JOSHUA E. SCHLIEDER⁷, MOLLY R. KOSIAREK^{13,†}, MAKENNAH BRISTOW⁸, ELISABETH NEWTON^{1,**}, MEGAN BEDELL⁹, DAVID W. LATHAM³, JESSIE L. CHRISTIANSEN⁵, GILBERT A. ESQUERDO³, PERRY BERLIND³, MICHAEL L. CALKINS³, AVI SHPORER¹, JENNIFER BURT¹, SARAH BALLARD¹, JOSEPH E. RODRIGUEZ³, NICHOLAS MEHRLE¹, COURTNEY D. DRESSING¹⁰, SARA SEAGER^{1,11}, JASON DITTMANN¹, DAVID BERARDO¹, LIZHOU SHA¹, ZAHRA ESSACK¹¹, ZHUCHANG ZHAN¹¹, MARTIN OWENS¹, ISABEL KAIN¹, JOHN H. LIVINGSTON¹², ERIK A. PETIGURA^{13,*}, ERICA J. GONZALES^{14,‡}, HOWARD ISAACSON¹⁰, ANDREW W. HOWARD¹³

ABSTRACT

We produce light curves for all $\sim 34,000$ targets observed with K2 in Campaign 17 (C17), identifying 34 planet candidates, 184 eclipsing binaries, and 222 other periodic variables. The forward-facing direction of the C17 field means follow-up can begin immediately now that the campaign has concluded and interesting targets have been identified. The C17 field has a large overlap with C6, so this latest campaign also offers a rare opportunity to study a large number of targets already observed in a previous K2 campaign. The timing of the C17 data release, shortly before science operations begin with the Transiting Exoplanet Survey Satellite (TESS), also lets us exercise some of the tools and methods developed for identification and dissemination of planet candidates from TESS. We find excellent agreement between these results and those identified using only K2-based tools. Among our planet candidates are several planet candidates with sizes $< 4R_{\oplus}$ and orbiting stars with $Kp \lesssim 10$ (indicating good RV targets of the sort TESS hopes to find) and a Jupiter-sized single-transit event around a star already hosting a 6 d planet candidate.

Subject headings: methods: data analysis, planets and satellites: detection, techniques: photometric

1. INTRODUCTION

Launched in 2009, the success of *Kepler* and its extended mission, K2, is unprecedented. In addition to their considerable contributions to other areas of astrophysics, these missions have led to planets candidates

and confirmed planets in the thousands (*Kepler*) and hundreds (*K2*). Unlike the original *Kepler* mission, K2 observes along the ecliptic plane, providing 30-minute-cadence light curves for several thousand targets in each roughly 80-day campaign (Howell et al. 2014).

The surge of data provided by the mission at the end of each campaign is processed and vetted for potential planet candidates. Due to spacecraft systematics and various sources of astrophysical variability, systems showing interesting signals are vetted by-eye before proceeding with additional confirmation follow-up with ground-based telescopes.

The recently launched Transiting Exoplanet Survey Satellite (TESS) will observe $\sim 90\%$ of the sky, approximately 400 times what *Kepler* observed and 26 times what K2 has observed so far. While experience shows that the vetting of potential planet candidates from K2 campaigns can be completed by a single person or a small team, the number of TESS candidates to be sifted may be far larger. Partly for that reason, TESS employs a larger and better-funded team that has been preparing a set of advanced diagnostics and tools. Because TESS observes in the anti-sun direction while orbiting the Earth (Ricker et al. 2014), if TESS candidates can be quickly identified after each sector, they can be immediately sent to ground-based observers to confirm the planets and study them in more detail.

The recent delivery of data from K2 Campaigns 16 and 17 (C16 and C17) have provided us with the chance to exercise some of the tools and techniques being developed for rapid planet candidate identification and dissemination from TESS and compare results to previous techniques used for K2. We conducted a rapid analysis of data from C16 using tools and methods developed

¹ Department of Physics, and Kavli Institute for Astrophysics and Space Research, Massachusetts Institute of Technology, Cambridge, MA 02139, USA

² Jet Propulsion Laboratory, California Institute of Technology, 4800 Oak Grove Drive, Pasadena, CA 91109, USA

³ Center for Astrophysics, 60 Garden Street, Cambridge, MA 02138, USA

⁴ Department of Physics and Astronomy, Tufts University, Medford, MA 02155, USA

⁵ Caltech/IPAC-NASA Exoplanet Science Institute, 770 S. Wilson Ave, Pasadena, CA 91106, USA

⁶ Département de Physique, Université de Montréal, Montréal, H3T 1J4, Canada

⁷ NASA Goddard Space Flight Center, 8800 Greenbelt Road, Greenbelt, MD 20771, USA

⁸ Department of Physics, University of North Carolina at Asheville, Asheville, NC 28804, USA

⁹ Center for Computational Astrophysics, Flatiron Institute, 162 5th Ave., New York, NY 10010, USA

¹⁰ Astronomy Department, University of California, Berkeley, CA, USA

¹¹ Department of Earth, Atmospheric and Planetary Sciences, Massachusetts Institute of Technology, Cambridge, MA 02139, USA

¹² Department of Astronomy, Graduate School of Science, The University of Tokyo, Hongo 7-3-1, Bunkyo-ku, Tokyo, 113-0033, Japan

¹³ Cahill Center for Astrophysics, California Institute of Technology, Pasadena, CA 91125, USA

¹⁴ Department of Astronomy and Astrophysics, University of California, Santa Cruz, CA 95064, USA

[†] NSF Graduate Research Fellow

^{**} NSF Postdoctoral Fellow

^{*} NASA Hubble Fellow

[‡] Texaco Fellow

strictly for K2 (Yu et al. 2018). With C17, we include a more TESS-like analysis using several of the tools and team members that will soon examine real TESS data.

C16 and C17 are also “TESS-like” in at least two other ways. First, these are both “forward-facing” campaigns in which the Earth-trailing K2 observed roughly anti-sun from the Earth; as with TESS sectors (see above), K2’s forward-facing fields can be immediately observed from the ground if identified with sufficient rapidity. Second, both of these fields partial overlap with previous K2 campaigns: C16 with C5 (observed April–July 2015) and C17 with C6 (July–September 2015). The rare overlap between C17 and C6 offers an opportunity to study for again a large number of targets previously observed by K2. Campaign 18, currently being observed, will also partly overlap C5 and C16. Similarly, repeated observations of the same targets will occur regularly when TESS begins near-continuous, year-long observations of the ecliptic poles.

Here, we present the techniques and results of our rapid identification of planet candidates and other astrophysical variables observed in C17. Sec. 2 details the identification process of planet candidates using methods and tools developed for both K2 and for TESS. Stellar and planet candidate parameters are discussed in Sec. 3. Sec. 4 discusses the results from the two independent vetting techniques described in Sec. 2. Similarities and discrepancies between planet candidates identified in C17 and C6 are discussed in Sec. 5. We remark on several individually-interesting systems in Sec. 6, and finally conclude in Sec. 7.

2. IDENTIFYING PLANET CANDIDATES

K2 observed C17 from March 1 until May 8, 2018. At 68 days, the campaign is slightly shorter than most previous K2 campaigns. We followed exactly the methods of Yu et al. (2018) to compute photometry and identify transit-like Threshold Crossing Events (TCEs). As soon as the raw cadence files were transferred from the spacecraft and uploaded to MAST, we downloaded these data and began our analysis. We converted raw K2 cadence data to target pixel files with `kadenza`¹⁹ (Barentsen & Cardoso 2018), converted pixel files to time-series photometry with `k2phot`²⁰, and identified TCEs in light curves using `TERRA`²¹ (Petigura 2015; Petigura et al. 2018). We have uploaded light curves for all C17 sources outside the Solar system in machine-readable format on the ExoFOP-K2 website²².

We identified 1274 TCEs with multi-event statistic (effectively a measure of signal-to-noise) ≥ 10 , and pursued two parallel paths to winnow down these 1274 TCEs to a list of reliable planet candidates. In one, we used a set of new tools being developed for efficient and robust vetting of candidates expected to be delivered soon by TESS; we hereafter refer to this as TESS-like candidate vetting. We also employed a so-called K2-like vetting approach by using a set of K2-specific tools and practices that have been refined through the past four years of K2 operations (Crossfield et al. 2015, 2016, 2017; Schlieder

et al. 2016; Obermeier et al. 2016; Sinukoff et al. 2016; Petigura et al. 2018; Ciardi et al. 2018; David et al. 2018; Yu et al. 2018). We outline both approaches below, and later compare the results of each in 4.1.

2.1. TESS-Like Vetting

In this effort we use the `TERRA` data products with the TESS Exoplanet Vetter (TEV), which is the web interface tool developed as part of the TESS Science Office data pipeline. TEV will be used to identify TESS Objects of Interest (TOIs) in the TCEs found in the TESS pipeline of record run by the Science Payload Operations Center (SPOC) at NASA/Ames and the internal Quick-Look Pipeline (QLP; Huang et al., in prep.) run at MIT. TEV was developed at MIT by the TESS Science Office staff, and will be described in more detail by Guerrero et al. (in prep.)

TEV imports a data delivery into a database and displays various vetting plots and data for the candidate TCEs for the first round of vetting by individuals. The data reduction pipeline that generated the analysis products — in this case `TERRA`, but SPOC or QLP for TESS science operations — provides an analysis summary page for each candidate TCE and a more comprehensive multi-page analysis report. The pipeline also provides a spreadsheet with the EPIC or TIC ID, and basic stellar and transit parameters.

During the individual vetting phase, human vetters inspect the light curve and other metrics in the analysis summary page (and extended report if necessary) to determine whether the candidate is a planet candidate (PC), eclipsing binary (EB), stellar variability (V), other astrophysical source of variability (O), instrument or systematic noise (IS), or undecided (U). For multi-planet systems, the candidates can be compared consecutively. Each individual vetter assigns a disposition to the candidate and has the option to make additional comments about the candidate. To complete the individual vetting stage, a candidate must get at least three unanimous individual dispositions or up to five total dispositions. The K2 C17 delivery had 1274 TCEs. A group of nineteen vetters completed the initial vetting stage in less than twenty-four hours after the delivery was imported into TEV.

TCEs classified unanimously as EB, V, or IS are automatically assigned that value as their final disposition. Targets classified unanimously as PC or with differing dispositions between vetters are flagged for group vetting, the second stage of the vetting process. Once the initial individual vetting concludes, group vetting begins by resolving conflicts for systems classified with at least one planet candidate or undecided disposition. Following this, the group inspects TCEs dispositioned unanimously as planet candidates. Conflicts between EB, V, and IS are resolved last. In this C17 exercise, the group applied and practices the conventions for assigning candidate dispositions that will be carried over to nominal TESS operations, including how to disposition and annotate contact binaries, candidates in a multi-transit system triggered by an eclipsing binary’s secondary eclipses, and candidates with radii $> 30R_{\oplus}$.

The group vetting process took about three hours to disposition 180 TCEs. This duration is not fixed, and is likely to evolve as TESS vetters are trained. Sys-

¹⁹ <https://github.com/KeplerGO/kadenza>

²⁰ <https://github.com/petigura/k2phot/>

²¹ <https://github.com/petigura/terra>

²² <https://exofop.ipac.caltech.edu/k2/>

tems identified in the exercise as known planets or eclipsing binaries were still dispositioned as PC, but in nominal TESS operations, TEV will filter candidates using catalogs of known planets, eclipsing binaries, and variable stars. Several of the candidates identified as strong candidates for observation were known targets in K2’s Campaign 6, which demonstrates that TEV users have the materials and expertise necessary to reliably identify planet candidates.

At the conclusion of group vetting, a TEV administrator closed the K2 C17 delivery to additional changes and TEV generated the final disposition list for download by TEV users. As in nominal TESS operations, the final C17 list was disseminated to the TESS Follow-Up Observing Program (TFOP²³).

Although we have endeavored to implement the full TESS vetting process, our K2 C17 vetting diagnostic products did not provide the full diagnostic capabilities that will be available from the SPOC and QLP pipelines for TESS vetting. First, no centroid shift information was available to aid in identifying nearby eclipsing binaries from the K2 data alone, on account of K2’s extremely high pointing jitter. Second, the K2 vetting diagnostics provided access to a light curve from only one photometric aperture per target. TESS pipelines will provide light curves from several aperture sizes to help to identify blended EB false positives. Third, the TESS analysis will implement ephemeris matching between the 2-minute-cadence postage stamps (a restricted set of targets) and the 30-minute-cadence full frame images (FFIs) to provide an additional means of identifying TESS aperture contamination by near or distant variable sources; we did not employ ephemeris matching in our C17 vetting. Finally, an extensive catalog of known variables and transit false positives is under development. TESS TCEs will be automatically cross-referenced to data in the catalog before the human vetting process begins, but since this catalog is not yet complete we did not cross-reference our C17 candidates against it.

2.2. K2-Like Vetting

Our K2-like vetting procedure closely followed previous efforts by our group (e.g., Yu et al. 2018). Six participants inspected a subset of TCEs that were assigned in order of TCE number (the EPIC ID appended by the candidate number). This pseudo-random scheme ensured that a given vetter inspected a sample of signals that covered a range of S/N. Each TCE was inspected by at least one person, and by the end of the vetting procedure 986 TCEs were inspected by 2 or more people (with 288 inspected by only one person). This resulted in 2548 individual dispositions for the 1274 TCEs, across 87 unique potential candidates.

Of these 87 signals, 45 were consistently identified as planet candidates by at least 2 people and 50 were identified as a candidate by at least one person without contest. While this vetting procedure was necessarily subjective, the common characteristics we looked for in the TERRA diagnostic plots in order to assign the disposition of a candidate were: consistent depth, no obvious odd/even variations in depth or transit time which might suggest an EB, lack of an obvious secondary eclipse, and lack of

significant phase-coherent out-of-transit variability. We did not penalize signals for being V-shaped alone. However, if a TCE was deep, V-shaped, and long in duration yet still lacked an obvious secondary eclipse, it was ultimately considered a planet candidate but flagged as a possible false positive. Finally, one vetter inspected each of the 87 flagged candidates and issued a final disposition.

The number of candidates that survived this final vetting stage was 53. The candidates that were demoted included 1 which was a duplicate of an accepted candidate, 19 which were deemed to be spurious (i.e. systematic artifacts) or otherwise failing to have a consistent shape and depth well above the photon noise, 2 which showed out-of-transit variability in phase with the signal in question (EPIC 212641218 and 212869892), and 12 which showed clear signs of being an EB, a duplicate of an EB signal (i.e. half or double the period), or having an ephemeris match to an EB. Finally, the candidates from the K2-like vetting were subjected to further cuts which are described in Sec. 4.1.

Close inspection of the light curves of the planet candidates revealed interesting information about a select number of candidates, which we summarize below in Sec. 6.

3. STELLAR AND PLANETARY CANDIDATE PARAMETERS

At the conclusion of the vetting exercises described above, we have two lists of possible planet candidates with only a few physical parameters known. Of these, the most salient are a candidate’s orbital period (shown in Fig. 1) along with transit depth and apparent stellar brightness (shown in Fig. 4). Stellar parameters for C17 stars are not available in the Ecliptic Planet Input Catalog (EPIC) as they were in past K2 campaigns (Huber et al. 2016), so the next step is to infer physical parameters such as radii and temperatures.

3.1. Ground-based Spectroscopy

Happily, EPIC parameters and ground-based stellar spectroscopy exist for some C17 stars also observed in C6. Dressing et al. (2017a) describe medium-resolution infrared spectroscopy of late-type systems using IRTF/SpeX, and Petigura et al. (2018) describe high-resolution optical spectroscopy with Keck/HIRES of a broader sample. Numerous spectra have also been acquired with the Tillinghast Reflector Echelle Spectrograph (TRES; Fűrész 2008) and uploaded to the ExoFOP-K2 website; we describe these observations below. Table 3 lists the key stellar parameters reported for 24 targets in C17 from SpeX, HIRES, and TRES. We also include parameters of two newly identified candidates orbiting bright stars from C17, EPIC 212628254 and 212779563.

TRES is located on the 1.5-m Tillinghast Reflector at Fred Lawrence Whipple Observatory on Mount Hopkins. TRES is a fiber-fed cross-dispersed echelle spectrograph with a resolving power of $R \approx 44,000$ and an instrumental velocity precision of 10 to 15 m s⁻¹, well-suited to stellar classification and identification of binaries via radial velocity variations and/or composite spectra. We use the Stellar Parameter Classification (SPC) package (see Buchhave et al. 2012) to determine the effective temper-

²³ <https://tess.mit.edu/followup/>

ature, surface gravity, metallicity, and rotational broadening of each spectrum, and we report those values in Table 3. We also report the radial velocities derived from the cross-correlation of a single spectral order against the best-matched synthetic spectrum, shifted to the absolute IAU scale. The TRES spectra—along with plots of stellar classifications resulting from cross-correlation against a coarse grid of synthetic spectra and spectral regions of interest—are available on ExoFOP-K2²⁴.

3.2. Multicolor Photometry and Gaia DR2

Despite the spectroscopic data from SpeX, HIRES, and TRES, we desire a complete and homogeneous set of stellar parameters against which to compare our C17 candidate sample. To this end, we set aside spectroscopic parameters and instead use EPIC multicolor (*BVugrizJHK*) photometry, parallaxes from Gaia DR2 (Gaia Collaboration et al. 2016, 2018), and isochrones²⁵ (Morton 2015) to derive stellar parameters using the MIST isochrones (Dotter 2016; Choi et al. 2016).

For C6 targets we use the Gaia-K2 cross-match from <https://gaia-kepler.fun>. For targets not in C6 we run our own cross-match between the EPIC locations and Gaia DR2 using an initial search radius of 5", selecting the Gaia source that most closely matches the position and magnitude of the K2 target. There were no ambiguous cases. All stars with $|Kp - G| > 0.5$ turned out to be stars where Kp was estimated from 2MASS colors alone. For all planet candidates, we are pleased to find that the distances inferred from isochrones are consistent with those from Gaia (at the 3σ level). The inferred stellar parameters for our candidates are listed in Table 2 and are online at ExoFOP-K2, and a color-magnitude diagram of our final candidate sample is shown in Fig. 2.

4. RESULTS AND DISCUSSION

4.1. Purifying the Sample

Some of the TCEs that we identified as planet candidates subsequently turned out to be non-planetary. Eleven candidates were identified as planet candidates during TESS-like group vetting, but were subsequently eliminated because the implied candidate radii would be $> 30R_{\oplus}$. These stars are EPIC 212579164, 212580081, 212627712, 212628098, 212770429, 212651213, 212757601, 212769367, 212769682, 212871068, and 212884586.

For the last of these, 212884586, Gaia DR2 shows two stars near the source’s location with $G=19.8$ and 19.6 mag, both located at distances >400 pc and both within the K2 aperture. Either could be the transit host and the transit would be diluted by the light of the other, in which case our inferred radius of $20_{-13}^{+21}R_{\oplus}$ would reach $\sim 30R_{\oplus}$. We therefore exclude this system from our planet candidate list.

We list EPIC 212658818 as an EB because its transit depth varies throughout the campaign, both in C17 and in C6. This variation is likely due to the putative transits occurring around a secondary star 12" to the south that is partly in the K2 aperture. Ground-based followup

photometry²⁶ indicates that this secondary star, fainter by 4.1 mag, is the true host of the eclipses (which have a depth of 42%).

We originally identified an EB and a planet candidate around EPIC 212651213 and 251810686, but then discovered that both EPIC stars target the same system (with an offset in the K2 data “postage stamp” for EPIC 251810686). We also acquired a light curve²⁷ confirming an event depth of 9% at our measured ephemeris. However, we remove both systems from our candidate list because this is a known quintuple system with two eclipsing binaries (Rappaport et al. 2016).

We note that several remaining candidates have radii formally below our $30R_{\oplus}$ limit, but are still grazing transits and so have large radius uncertainties (e.g., 212628477 and 212686312). As currently formulated, the TESS vetting process would report these as candidates, so we retain them in our C17 sample with a note in Table 2.

4.2. Planet Candidates, EBs, and Variables

Our TESS-like vetting identified 34 planet candidates, all of which were marked as candidates in K2-like vetting. Our standard K2 vetting process identified 53 planet candidates, but several of these were not marked as candidates in TESS-like vetting for reasons including:

- 251504891.01: Marked as variable because of coherent out-of-transit variation.
- 212473154.01: Marked as EB because the candidate radius $R_C = 65R_{\oplus}$.
- 212789681.01: Marked as EB because the transit duration $T_{14} = 0.12$ d is a large fraction of $P = 0.49$ d.
- 212421319.01: Marked as EB because the odd and even transits have different depths.
- 212499716.01: Marked as EB because of a faint secondary eclipse, seen more clearly in C6 photometry.
- 212579164.01: Marked as EB because $R_C = 46R_{\oplus}$.
- 212580081.01: Marked as EB because $R_C = 35R_{\oplus}$.
- 212627712.01: Marked as IS because the K2 photometric aperture mostly captures light from a nearby, brighter star.
- 229228115.01: Marked as EB because $T_{14} = 0.13$ d is a large fraction of $P = 0.55$ d.
- 212705192.01: Marked as EB because of odd-even effect, and because Keck/HIRES and TRES spectra show the star to be double-lined.
- 212740148.01: Marked as EB because of a faint secondary eclipse. Also, the K2 photometric aperture mostly captures light from a nearby, brighter star.

²⁶ https://exofop.ipac.caltech.edu/k2/edit_target.php?id=212658818

²⁷ https://exofop.ipac.caltech.edu/k2/edit_target.php?id=212651213

²⁴ <https://www.exofop.ipac.caltech.edu/k2>

²⁵ <https://github.com/timothydmorton/isochrones/>

- 212770429.01: Marked as IS because the K2 photometric aperture mostly captures light from a nearby, brighter star.

Table 2 lists the basic parameters for our final list of 34 planet candidates from K2’s C17. The properties of this population are also summarized in Fig. 1 (orbital periods), Fig. 3 (phase-folded candidate light curves), Fig. 4 (Kp and transit depth), and Fig. 5 (candidate radius and insolation).

We also include a list of all likely EBs and other apparently astrophysical variables identified from our TESS-like analysis. A total of 184 EBs are listed in Table 4, and 222 variables are listed in Table 5. These tables also include the final comments (if any) assigned to each TCE during the group vetting process. Note also that the numbers above likely somewhat overestimate the objects in each category, since EBs with secondary eclipses and variables with multiple harmonics are both often identified as multiple TCEs in the same system.

5. COMPARING PLANET CANDIDATES: C17 VS. C6

Twenty-one of our planet candidates (orbiting 18 stars) were also observed by K2 in C6. This earlier campaign was searched for transiting planets by many groups, giving us a rare opportunity to compare the results of these analyses. Different teams have used a variety of photometric and transit search pipelines, all using fully calibrated data products. Because our analysis here uses raw cadence data (calibrated only by *kadenza*), our noise levels are higher and we do not expect to identify all transit-like signals described in the literature. Although we might naively expect substantial or complete overlap between the C6 surveys, that is not what we find. Table 1 compares the disposition of these 21 C6+C17 candidates by several large-scale surveys, which we describe below.

Pope et al. (2016) identify 19 of our candidates as planet candidates, missing only two of our candidate systems — EPIC 212634172 and 212686205. This is the highest degree of overlap for any C6 catalog, suggesting a higher completeness rate than other analyses.

Dressing et al. (2017a); ? derive stellar and planetary parameters and associated false positive probabilities for planets orbiting late-type stars that were discovered by multiple transit surveys. They validate EPIC 212554013 and 212686205, leave 212634172 as a planet candidate, and deem 212572452 to be a false positive because its photometry is blended with that of 212572439.

Mayo et al. (2018) identify and validate planets in ten of our candidate systems: EPIC 212496592, 212521166, 212580872, 212686205, 212689874, 212697709, 212735333, 212768333, 212779596, and 212803289. They do not report any candidates around our candidate systems EPIC 212554013, 212570977, 212572452, 212572439, 212575828, 212634172, 212661144, or 212813907.

Finally, the signals in 11 of our C6+C17 systems were identified as planet candidates by Petigura et al. (2018), *viz.*, EPIC 212521166, 212554013, 212570977, 212572452, 212572439, 212580872, 212689874, 212697709, 212735333, 212779596, and 212803289. In a follow-up paper, Livingston et al. (submitted) validate EPIC 212521166, 212554013, 212580872, 212689874, and 212779596. EPIC 212697709 remains

a candidate in the latter paper with a false positive probability of 1.9%, but this planet was validated as WASP-157 (Močnik et al. 2016). Livingston et al. also find a sufficiently low FPP to validate EPIC 212803289 and 212570977, but out of an abundance of caution they deem these to be candidates because of their large radii ($> 10R_{\oplus}$). They also find EPIC 212572439 and 2127355333 to have very low FPPs but call these merely candidates because of an additional stellar source in the K2 photometric aperture (Gonzales et al., in prep.).

As a further comparison, we calculated the ephemerides offsets of eleven of our C17 candidates with those derived from C6 data. To avoid possible biases that could arise from using different pipelines, we only compared those candidates with ephemerides reported by Livingston et al. (submitted). Ephemerides for all eleven candidates are consistent at the 3σ level, with only three candidates disagreeing at the $2-3\sigma$ level (212570977.01, 212779596.01, and 212803289.01).

6. INDIVIDUAL SYSTEMS

Below we discuss several interesting individual systems discovered by our C17 analysis. We separate these into several groups: potentially exciting discoveries warranting additional follow-up observations; more generic candidates nonetheless requiring some additional discussion; and finally, objects which (though planet candidates) may be somewhat more likely to be non-planetary false positives.

- 212779563 (Wolf 503, HIP 67285). This candidate planet’s size of $2R_{\oplus}$ lies near the gap between sub-Neptunes and super-Earths (Fulton et al. 2017). The short period and nearby, bright star ($V=10.3$, $H=7.8$) could make this an excellent target for future RV and transmission spectroscopy. This system is described in more detail by Peterson et al. (submitted).
- 212628254 (HD 119130). This $2.7R_{\oplus}$ candidate orbits a $V=9.9$, slightly evolved G star. It may also be a good RV target because of the planet’s moderate size and bright host star.
- 212813907: In addition to the transiting planet candidate reported here with $P = 6.7$ d, we see an obvious single transit with depth 1.8% centered at $\text{BJD}_{\text{TBD}}=2458213.82646$ and with duration 0.66 d. This points to a candidate transiting companion with a radius of $\sim 1R_{\text{Jup}}$ and $P \approx 1000$ d. No corresponding transit was seen for this star during C6.
- 212686205 (K2-128). (Dressing et al. 2017a) showed that this star is a K4 dwarf, despite its EPIC classification as a giant (Huber et al. 2016). The star exhibits semi-sinusoidal brightness variations that are likely due to starspots and stellar surface rotation, with a period of $P_{\text{rot}}=11.9$ days and amplitude of 0.018 mag. The position of the star in a rotation period-color diagram indicates an age similar to that of Praesepe ($\sim 600-800$ Myr).
- 212768333: This candidate was validated as the single-planet K2-198 b ($P = 17$ d) using data from

TABLE 1
OUR C17 CANDIDATES OBSERVED IN C6

| Candidate | C6 | Po16 | Ma18 | Pe18 | Li18 | Name | Validation Reference / Note |
|--------------|----|------|------|------|------|-----------|-----------------------------|
| 212496592.01 | Y | PC | VP | N | N | K2-191b | Mayo et al. (2018) |
| 212521166.01 | Y | PC | VP | PC | VP | K2-110b | Osborn et al. (2017) |
| 212554013.01 | Y | PC | N | PC | VP | K2-127b | Dressing et al. (2017b) |
| 212570977.01 | Y | PC | N | PC | PC | — | — |
| 212572439.01 | Y | PC | N | PC | PC | — | Blend with 212572452. |
| 212572452.01 | Y | PC | N | N | PC | — | Blend with 212572439. |
| 212575828.01 | Y | PC | N | N | N | — | — |
| 212580872.01 | Y | PC | VP | PC | VP | K2-193 | Mayo et al. (2018) |
| 212634172.01 | Y | N | N | N | N | — | — |
| 212661144.01 | Y | PC | N | N | N | — | — |
| 212686205.01 | Y | N | VP | N | N | K2-128b | Dressing et al. (2017b) |
| 212689874.01 | Y | PC | VP | PC | VP | K2-195b | Mayo et al. (2018) |
| 212689874.02 | Y | PC | VP | PC | VP | K2-195c | Mayo et al. (2018) |
| 212697709.01 | Y | PC | VP | PC | PC | WASP-157b | Močnik et al. (2016) |
| 212735333.01 | Y | PC | VP | PC | PC | K2-197b | Mayo et al. (2018) |
| 212768333.01 | Y | PC | VP | N | N | K2-198b | Mayo et al. (2018) |
| 212768333.02 | Y | PC | N | N | N | — | — |
| 212779596.01 | Y | PC | VP | PC | VP | K2-199b | Mayo et al. (2018) |
| 212779596.02 | Y | PC | VP | PC | VP | K2-199c | Mayo et al. (2018) |
| 212803289.01 | Y | PC | VP | PC | PC | K2-99b | Smith et al. (2017) |
| 212813907.01 | Y | PC | N | N | N | — | — |

References: Po16 (Pope et al. 2016), Ma18 (Mayo et al. 2018), Pe18 (Petigura et al. 2018), Li18 (Livingston et al., submitted).

Notes: VP (validated planet), PC (planet candidate), N (not identified).

C6 (Mayo et al. 2018), but our C17 data also reveal a second candidate with $P = 7.4$ d. These two candidates, plus a third ($P = 3.4$ d) were previously reported by Pope et al. (2016). The star has K2 data available from Campaigns 6 and 17, making a search for additional transiting planets at longer orbital periods possible. The star shows periodic variability which is likely due to rotation of the spotted surface. The inferred rotation period of 7.02 days and variability amplitude of 0.024 mag (from the 10th to 90th percentile) point to a young system age (Rebull et al. 2016, 2018), likely older than the Pleiades (125 Myr) but perhaps younger than or similar in age to Praesepe (~ 600 –800 Myr).

- 212619190 and 212707574: These are both ultra-short-period (USP) planet candidates. While the signals are convincing, the inferred sizes we report here are larger than typical USPs (Winn et al. 2018).

The following planet candidates seem reliable but warrant some additional discussion.

- 212748535 – We originally identified this candidate as a signal associated with EPIC 212748598 ($Kp=17.4$ mag). This faint source is classified as a galaxy by The 2dF Galaxy Redshift Survey (Colless et al. 2001) and appears galaxy-like in Pan-Starrs multicolor imaging (A. Rest, private communication). We conclude that EPIC 212748598 is a galaxy despite its designation as “STAR” in EPIC. Gaia DR2 shows a brighter, stellar source with $\Delta G = 5.4$ mag within our K2 aperture and $20''$ away. This brighter star is EPIC 212748535, which Gaia shows to be a K dwarf ($T_{\text{eff}}=3800$ K, $R_* = 0.67R_{\odot}$) and which dominates the flux in our K2 photometric aperture. We conclude that the

brighter source, EPIC 212748535, is the true host of the observed ~ 1 mmag transit.

- 212682254: This star has a candidate with $R_C = 6R_{\oplus}$ and $P = 10.7$ d, and also shows photometric variability due to starspots, with an amplitude of 0.019 mag (again measured from the 10th to 90th percentile) and an inferred rotation period of 9.45 days. The rotation period and color place the star near the slowly-rotating I-sequence of Praesepe members (Barnes 2007), indicating an age similar to that cluster (~ 600 –800 Myr).
- 212572439 and 212572452: Our analysis independently identified two candidates with the same periods around these adjacent stars (separated by $6''$). A transit-like signal from the blend of these two sources has also been identified in previous works (Dressing et al. 2017b; Petigura et al. 2018, Livingston et al., submitted; Gonzales et al., in prep.), and both signals were identified (though the blend went unremarked) by Pope et al. (2016). Based on our inferred stellar and planetary properties, this signal could still be a transiting planet regardless of which of these two stars it orbits; we thus retain both signals as planet candidates. Additional follow-up will be required to identify which object is the transit host.

Finally, the objects below pass our criteria as planet candidates but show warning signs hinting that they may be non-planetary:

- 251590700: This source has no Gaia DR2 parallax so the derived stellar parameters are somewhat less certain. The parallax measurement is presumably lacking because of an enormous amount of excess noise in the five-parameter Gaia solution (`astrometric_excess_noise_sig=64781`),

suggesting the possibility that the star is a binary. Our transit fit implies a stellar density (assuming a circular orbit; Seager & Mallén-Ornelas 2003) of $\rho_{*,circ} = 0.0033^{+0.0005}_{-0.0003} \text{ g cm}^{-3}$, implying either a highly eccentric orbit or a false positive caused by an eclipsed, low-density giant star.

- 251582120: We originally identified this event as a signal around EPIC 251581990, a faint ($Kp=18.5$ mag) source listed as an “EXTENDED” (i.e., non-stellar) object in EPIC. Our aperture for this faint target enclosed another nearby brighter stellar source, EPIC 251582120 ($Kp=15.2$ mag), whose flux dominates our light curve. Our light curve fit for this brighter source implies $\rho_{*,circ} = 0.165 \pm 0.055 \text{ g cm}^{-3}$, mildly inconsistent with our **isochrones**+Gaia-derived stellar density of $0.79 \pm 0.20 \text{ g cm}^{-3}$. The crowded aperture and mismatch in stellar densities hint that this planet candidate may be less reliable.
- 212686312: This signal is both deep and V-shaped, indicating a grazing transit. Combined with the very short orbital period and the inferred companion radius presented here, the planetary nature of the signal is doubtful.
- 212628477: This star is rapidly rotating, with a period of 2.685 days and a variability amplitude of 0.045 mag. The star’s rapid rotation combined with its color suggest an age younger than that of the Pleiades (Rebull et al. 2016). The rotation period is clearly distinct from the much longer period of the planet candidate ($P=15.4$ d), but there are several warning signs for this candidate: the transits are grazing so the inferred companion is large ($21.0^{+15.4}_{-2.2} R_{\oplus}$); Gaia DR2 reports a highly uncertain radial velocity of $20.98 \pm 19.55 \text{ km s}^{-1}$, perhaps indicative of RV variability; and the TRES spectrum shows a probable shoulder in the cross-correlation function indicating a double-lined spectrum (see Table 3).
- 251539584 and 251539609: These two stars are both spectroscopic binaries. Both showed candidate transit signals with the same transit ephemeris ($P = 1.09$ d). The stars are roughly equal brightness ($\Delta Kp=0.2$ mag) and are separated by roughly $14''$ and are both contained in the photometric aperture applied to the other. The two stars are apparently associated and co-moving, based on their kinematics from Gaia DR2. The combined light curve is variable, indicating a rotation period of 4.34 days and amplitude of 0.002 mag (though the true amplitude must be larger because of flux dilution from the companion). TRES spectroscopy shows that both EPIC sources are short-period double-lined spectroscopic binaries (see Table 3), so we list these systems as candidate EBs.

7. DISCUSSION AND CONCLUSION

From $\sim 34,000$ stars observed in K2’s most recent field, Campaign 17, we identified 1274 transit-like events. Among these, we find 34 planet candidates (Table 2), 184

eclipsing binaries (Table 4), and 222 other periodic variables (Table 5). Because C17 was observed in “forward-facing” mode by K2 in its Earth-trailing orbit, these targets can be immediately observed before the ecliptic field sets for the season. Many of these objects were also observed by K2 during C6, offering a rare opportunity to study the same systems over a 1000 day timespan. Multiple observations of the same field will be commonplace when TESS begins near-continuous observations of the ecliptic poles, which will substantially increase that survey’s sensitivity to long-period planets. Though beyond the scope of this work, a comprehensive transit search in C6+C17 (or C5+C16) would probe a single, narrow range of orbital periods from 880–1030 d (and harmonics of these periods).

We evaluated the overlap between our C17 planet candidates and those observed in C6 by several earlier planet surveys, finding again that K2 efforts have substantially different completeness (Crossfield et al. 2016; Mayo et al. 2018). The C6 catalog of Pope et al. (2016) overlaps most closely with our C17 candidate list, indicating that that sample has either a high degree of completeness or (at worst) a very similar set of biases to that of our sample. Unfortunately, the different samples and data quality between the calibrated C6 data and our use of C17’s raw cadence data precludes any conclusions about false positive rates in these surveys. Nonetheless, the generally incomplete overlap between the candidate lists of different surveys lends support to the TESS science plan to use two independent pipelines, SPOC and QLP, to minimize the chances of interesting planet candidates passing unnoticed.

In this work we focus on the search for new transiting planet candidates, whose parameters are summarized in Table 2. We find several candidates that have sizes $< 4R_{\oplus}$ and orbit stars with $Kp \lesssim 10$, indicating that these are good RV targets. The most interesting are Wolf 503 (EPIC 212779563.01; see Peterson et al., submitted) and HD 119130 (EPIC 212628254.01). If found by TESS, such planet candidates would be ideal targets for fulfilling its prime science goal of contributing to the measured masses of 50 small planets.

Several other planet candidate discoveries highlight potentially intriguing dynamical and/or multi-body systems. We see a single, deep transit around EPIC 212813907, which also hosts a 6 d planet candidate, suggesting a Jupiter-sized companion on a long-period orbit. We also identify a candidate planet in each of two possible binary systems (EPIC 251539584 & 251539609, and EPIC 212572439 & 212572452).

In conclusion, K2’s rapid data releases for its recent campaigns have facilitated quick identification of many interesting astrophysical phenomena in time for immediate ground-based follow-up. This approach is qualitatively the same as that planned for TESS. In this C17 exercise, our TESS-like and K2-like vetting approaches both yielded the same set of planet candidates. This result validates the results derived from similar, past analyses of K2 and also demonstrates that the team members soon to be examining TESS data have the tools and expertise necessary for a successful mission. After four years *Kepler* yielded to *K2*; another four years on, in Olympic fashion *K2* will likewise pass the baton to *TESS* to continue building on the great legacy of exo-

planet exploration.

We thank A. Rest for discussions about the nature of EPIC 212748598.

I.J.M.C. acknowledges support from NASA through K2GO grant 80NSSC18K0308 and from NSF through grant AST-1824644.

This paper includes data collected by the *Kepler* mission. Funding for the *Kepler* mission is provided by the NASA Science Mission directorate. Some of the data presented in this paper were obtained from the Mikulski Archive for Space Telescopes (MAST). STScI is operated by the Association of Universities for Research in Astronomy, Inc., under NASA contract NAS5-26555. Support for MAST for non-HST data is provided by the NASA Office of Space Science via grant NNX13AC07G and by other grants and contracts. This research has made use of the Exoplanet Follow-up Observing Program (ExoFOP), which is operated by the California Institute of Technology, under contract with the National Aeronautics and Space Administration.

Facilities: Kepler, K2, FLWO:1.5m (TRES), KeckI (HIRES), APF (Levy)

REFERENCES

Barentsen, G., & Cardoso, J. V. d. M. 2018, Kadenza: Kepler/K2 Raw Cadence Data Reader, Astrophysics Source Code Library, 1803.005, ADS

Barnes, S. A. 2007, *ApJ*, 669, 1167, ADS, 0704.3068

Buchhave, L. A. et al. 2012, *Nature*, 486, 375, ADS

Choi, J., Dotter, A., Conroy, C., Cantiello, M., Paxton, B., & Johnson, B. D. 2016, *ApJ*, 823, 102, ADS, 1604.08592

Ciardi, D. R. et al. 2018, *AJ*, 155, 10, ADS, 1709.10398

Colless, M. et al. 2001, *MNRAS*, 328, 1039, ADS, astro-ph/0106498

Crossfield, I. J. M. et al. 2017, *AJ*, 153, 255, ADS, 1701.03811

—. 2016, *ApJS*, 226, 7, ADS, 1607.05263

—. 2015, *ApJ*, 804, 10, ADS, 1501.03798

David, T. J. et al. 2018, *AJ*, 155, 222, ADS, 1803.05056

Dotter, A. 2016, *ApJS*, 222, 8, ADS, 1601.05144

Dressing, C. D., Newton, E. R., Schlieder, J. E., Charbonneau, D., Knutson, H. A., Vanderburg, A., & Sinukoff, E. 2017a, *ApJ*, 836, 167, ADS, 1701.00586

Dressing, C. D. et al. 2017b, *ArXiv e-prints*, ADS, 1703.07416

Fűrész, G. 2008, PhD thesis

Fulton, B. J. et al. 2017, *AJ*, 154, 109, ADS, 1703.10375

Gaia Collaboration, Brown, A. G. A., Vallenari, A., Prusti, T., de Bruijne, J. H. J., Babusiaux, C., & Bailer-Jones, C. A. L. 2018, *ArXiv e-prints*, ADS, 1804.09365

Gaia Collaboration et al. 2016, *A&A*, 595, A1, ADS, 1609.04153

Howell, S. B. et al. 2014, *PASP*, 126, 398, ADS, 1402.5163

Huber, D. et al. 2016, *ApJS*, 224, 2, ADS, 1512.02643

Mayo, A. W. et al. 2018, *ArXiv e-prints*, ADS, 1802.05277

Morton, T. D. 2015, *isochrones: Stellar model grid package*, Astrophysics Source Code Library, 1503.010, ADS

Močnik, T. et al. 2016, *PASP*, 128, 124403, ADS, 1603.05638

Nidever, D. L., Marcy, G. W., Butler, R. P., Fischer, D. A., & Vogt, S. S. 2002, *ApJS*, 141, 503, ADS, astro-ph/0112477

Obermeier, C. et al. 2016, *ArXiv e-prints*, ADS, 1608.04760

Osborn, H. P. et al. 2017, *A&A*, 604, A19, ADS, 1605.04291

Petigura, E. A. 2015, *ArXiv e-prints*, ADS, 1510.03902

Petigura, E. A. et al. 2018, *AJ*, 155, 21, ADS, 1711.06377

Pope, B. J. S., Parviainen, H., & Aigrain, S. 2016, *MNRAS*, 461, 3399, ADS, 1606.01264

Rappaport, S. et al. 2016, *MNRAS*, 462, 1812, ADS, 1606.06324

Rebull, L. M. et al. 2016, *AJ*, 152, 114, ADS, 1606.00055

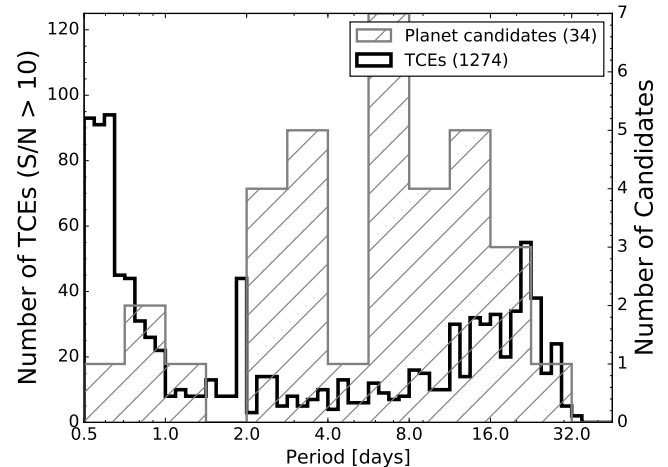


FIG. 1.— Orbital periods of planet candidates identified in our analysis. The dark, narrow-binned histogram (axis at left) shows the Threshold-Crossing Events (TCEs) identified by TERRA with $S/N \geq 10$ (see Sec. 2). The gray, hatched histogram (axis at right) indicates the distribution of 34 planet candidates.

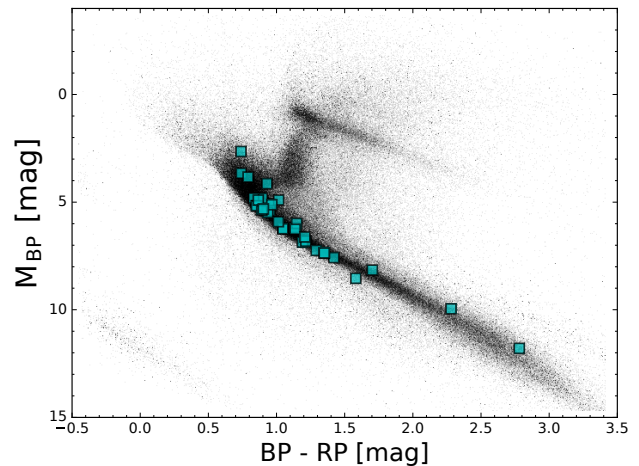


FIG. 2.— Color-magnitude diagram for our C17 planet candidates (squares) and for all K2 targets (gray background).

Rebull, L. M., Stauffer, J. R., Cody, A. M., Hillenbrand, L. A., David, T. J., & Pinsonneault, M. 2018, *AJ*, 155, 196, ADS, 1803.04440

Ricker, G. R. et al. 2014, in *Society of Photo-Optical Instrumentation Engineers (SPIE) Conference Series*, Vol. 9143, Society of Photo-Optical Instrumentation Engineers (SPIE) Conference Series, 20, 1406.0151, ADS

Schlieder, J. E. et al. 2016, *ApJ*, 818, 87, ADS, 1601.02706

Seager, S., & Mallén-Ornelas, G. 2003, *ApJ*, 585, 1038, ADS, arXiv:astro-ph/0206228

Sinukoff, E. et al. 2016, *ApJ*, 827, 78, ADS, 1511.09213

Smith, A. M. S. et al. 2017, *MNRAS*, 464, 2708, ADS, 1609.00239

Winn, J. N., Sanchis-Ojeda, R., & Rappaport, S. 2018, *ArXiv e-prints*, ADS, 1803.03303

Yu, L. et al. 2018, *ArXiv e-prints*, ADS, 1803.04091

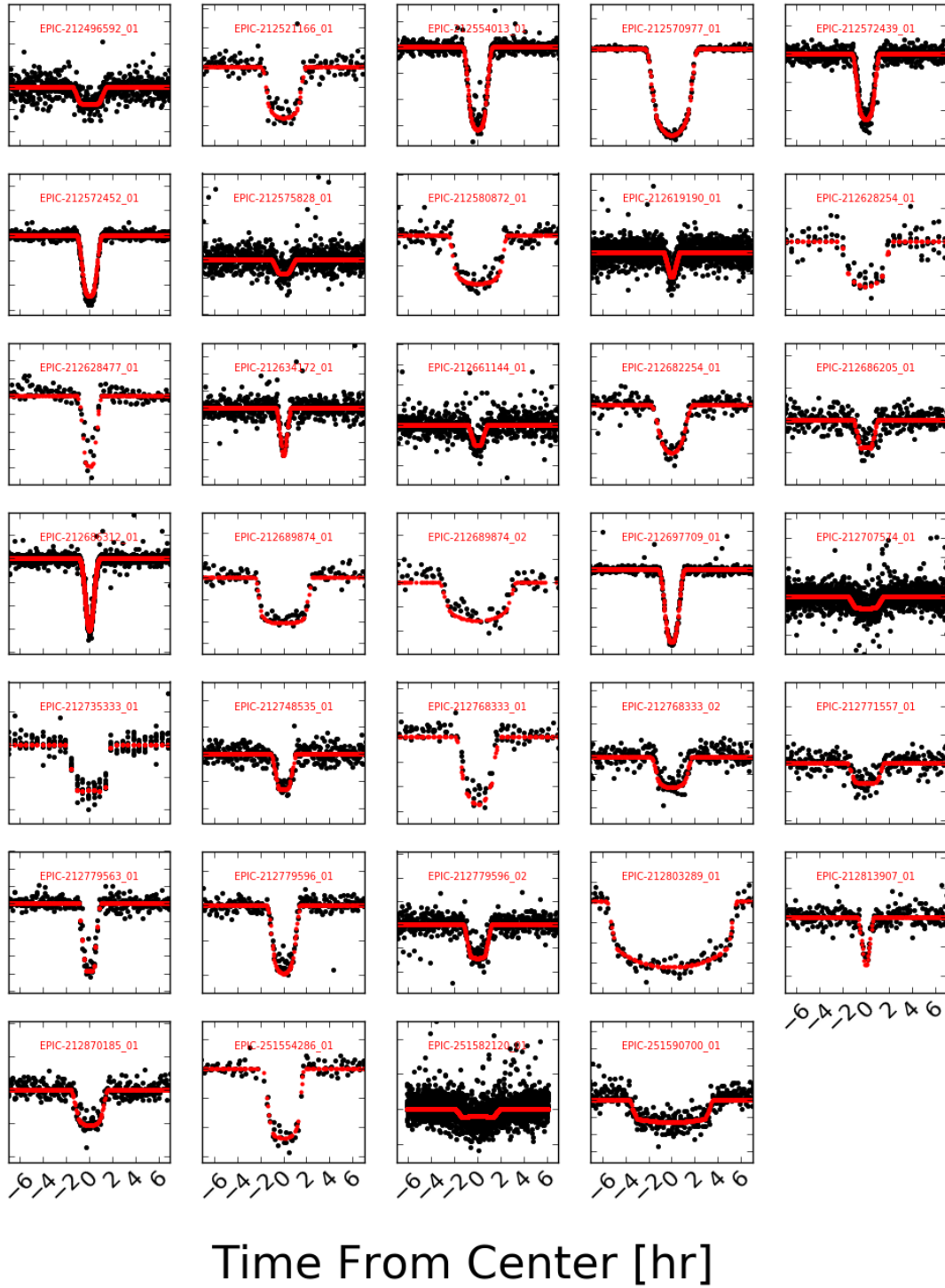


FIG. 3.— Phase-folded light curves of our 34 planet candidates, and their best-fit transit models. To show all transits, the vertical scale is different in each panel; system parameters are listed in Table 2.

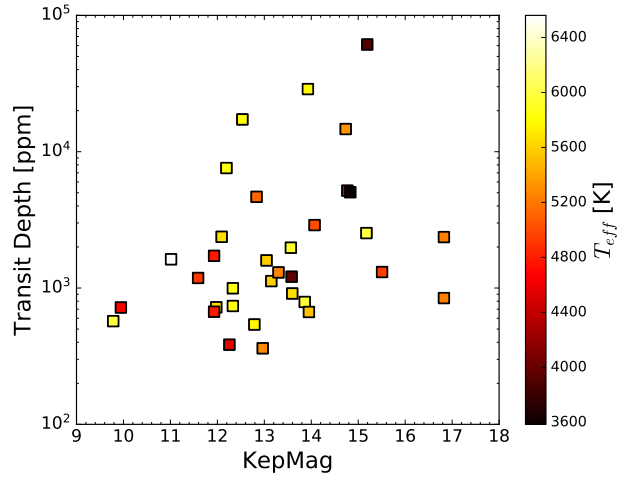


FIG. 4.— Transit depth and stellar magnitude for our planet candidates, as a function of stellar T_{eff} (color scale). The two brightest targets are Wolf 503 (EPIC 212779563) and HD 119130 (EPIC 212628254).

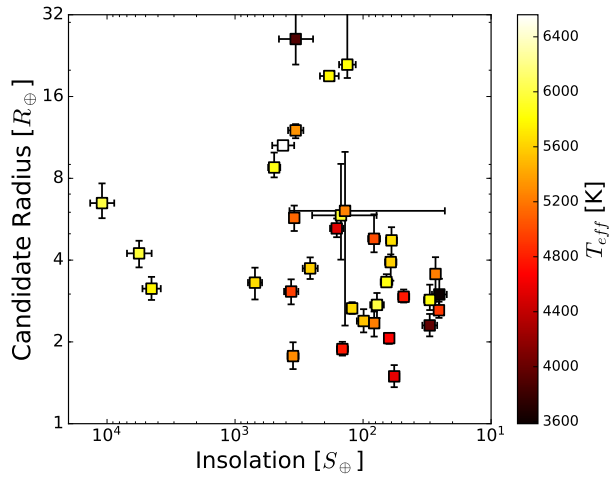


FIG. 5.— Candidate radius and incident insolation for our planet candidates, as a function of stellar T_{eff} (color scale).

TABLE 2
PLANET CANDIDATES FROM C17

| Candidate | K _p [mag] | P [d] | T ₀ BJD _{TDB} - 2454833 | T ₁₄ [hr] | R _p /R _* [%] | R _* [R _☉] | T _{eff} [K] | R _p [R _☉] | S _{inc} [S _☉] | Notes |
|--------------|-------------------------|---|--|--|---|-------------------------------------|-------------------------|---|---------------------------------------|--------------------------------------|
| 212496592.01 | 12.966 | 2.85883 ^{+0.00039} _{-0.00038} | 3347.02222 ^{+0.00047} _{-0.00053} | 2.17 ^{+0.40} _{-0.095} | 1.89 ^{+0.23} _{-0.20} | 0.86 | 5284 | 1.77 ^{+0.22} _{-0.19} | 352 | K2-191b (Mayo et al. 2018) |
| 212521166.01 | 11.590 | 13.8642 ^{+0.0011} _{-0.0011} | 3357.3269 ^{+0.0028} _{-0.0028} | 3.26 ^{+0.24} _{-0.27} | 3.35 ^{+0.25} _{-0.16} | 0.72 | 4915 | 2.62 ^{+0.20} _{-0.16} | 25.5 | K2-110b (Osborn et al. 2017) |
| 212554013.01 | 14.733 | 3.588223 ^{+0.00046} _{-0.00046} | 3348.97026 ^{+0.00046} _{-0.00046} | 2.137 ^{+0.086} _{-0.053} | 11.61 ^{+0.47} _{-0.59} | 0.95 | 5324 | 12.01 ^{+0.65} _{-0.63} | 336 | K2-127b (Dressing et al. 2017b) |
| 212570977.01 | 13.928 | 8.853181 ^{+0.00031} _{-0.00031} | 3347.02423 ^{+0.00021} _{-0.00021} | 4.192 ^{+0.23} _{-0.027} | 15.33 ^{+0.29} _{-0.15} | 1.14 | 5774 | 19.04 ^{+0.62} _{-0.62} | 183 | — |
| 212572439.01 | 12.835 | 2.581446 ^{+0.00038} _{-0.00038} | 3347.75306 ^{+0.00055} _{-0.00055} | 1.81 ^{+0.12} _{-0.036} | 6.17 ^{+0.67} _{-0.61} | 0.85 | 5124 | 5.72 ^{+0.63} _{-0.60} | 344 | Blend with 212572452 |
| 212572452.01 | 14.769 | 2.581446 ^{+0.00019} _{-0.00019} | 3347.75323 ^{+0.00030} _{-0.00030} | 1.761 ^{+0.036} _{-0.039} | 7.19 ^{+0.61} _{-0.50} | 0.67 | 4535 | 5.23 ^{+0.46} _{-0.38} | 160 | Blend with 212572439 |
| 212575828.01 | 15.508 | 2.06033 ^{+0.00018} _{-0.00018} | 3347.0331 ^{+0.00033} _{-0.00033} | 1.55 ^{+0.27} _{-0.37} | 3.71 ^{+0.38} _{-0.37} | 0.76 | 4949 | 3.07 ^{+0.33} _{-0.32} | 364 | — |
| 212580872.01 | 13.047 | 14.7881 ^{+0.0013} _{-0.0013} | 3352.4604 ^{+0.0029} _{-0.0029} | 4.34 ^{+0.14} _{-0.14} | 3.70 ^{+0.24} _{-0.24} | 0.98 | 5586 | 3.93 ^{+0.26} _{-0.26} | 60.8 | K2-193b (Mayo et al. 2018) |
| 212619190.01 | 12.788 | 0.911861 ^{+0.00032} _{-0.00032} | 3347.2783 ^{+0.0019} _{-0.0019} | 0.772 ^{+0.121} _{-0.121} | 2.33 ^{+0.24} _{-0.24} | 1.23 | 5765 | 3.14 ^{+0.37} _{-0.29} | 4494 | HD 119130 |
| 212628254.01 | 9.782 | 16.9813 ^{+0.00022} _{-0.00022} | 3347.2910 ^{+0.0044} _{-0.0044} | 3.69 ^{+0.59} _{-0.31} | 2.32 ^{+0.24} _{-0.24} | 1.08 | 5998 | 2.74 ^{+0.29} _{-0.29} | 77.9 | — |
| 212628477.01 | 12.533 | 15.42404 ^{+0.00081} _{-0.00081} | 3347.7248 ^{+0.0020} _{-0.0020} | 1.54 ^{+0.26} _{-0.23} | 13.8 ^{+0.2} _{-1.4} | 1.39 | 5823 | 21.0 ^{+0.2} _{-2.2} | 132 | Grazing transit |
| 212634172.01 | 14.831 | 2.851770 ^{+0.00083} _{-0.00083} | 3348.4657 ^{+0.0013} _{-0.0013} | 0.721 ^{+0.140} _{-0.062} | 7.27 ^{+0.98} _{-0.64} | 0.38 | 3585 | 2.99 ^{+0.42} _{-0.30} | 25.4 | — |
| 212661144.01 | 13.595 | 2.45875 ^{+0.00022} _{-0.00022} | 3347.2747 ^{+0.0028} _{-0.0028} | 1.10 ^{+0.29} _{-0.38} | 3.10 ^{+0.41} _{-0.41} | 0.98 | 5647 | 3.30 ^{+0.45} _{-0.44} | 698 | — |
| 212682254.01 | 13.565 | 10.70070 ^{+0.00088} _{-0.00088} | 3353.1746 ^{+0.0021} _{-0.0021} | 3.23 ^{+0.34} _{-0.34} | 4.74 ^{+0.23} _{-0.23} | 1.12 | 5936 | 5.8 ^{+1.8} _{-1.8} | 148 | — |
| 212682254.01 | 12.256 | 5.67623 ^{+0.00042} _{-0.00042} | 3347.6471 ^{+0.0044} _{-0.0044} | 1.45 ^{+0.21} _{-0.21} | 2.05 ^{+0.20} _{-0.20} | 0.67 | 4566 | 1.49 ^{+0.15} _{-0.13} | 57.1 | K2-128b (Dressing et al. 2017b) |
| 212686312.01 | 15.192 | 0.7476280 ^{+0.00056} _{-0.00056} | 3346.76330 ^{+0.00015} _{-0.00015} | 1.434 ^{+0.079} _{-0.067} | 45.4 ^{+0.8} _{-1.1} | 0.53 | 3904 | 26.0 ^{+0.23} _{-5.1} | 335 | Grazing transit |
| 212689874.01 | 12.330 | 15.8537 ^{+0.0013} _{-0.0013} | 3359.2217 ^{+0.0024} _{-0.0024} | 4.52 ^{+0.21} _{-0.15} | 3.11 ^{+0.12} _{-0.12} | 0.98 | 5842 | 3.32 ^{+0.23} _{-0.14} | 65.7 | K2-195b (Mayo et al. 2018) |
| 212689874.02 | 12.330 | 28.4545 ^{+0.0034} _{-0.0034} | 3349.1480 ^{+0.0044} _{-0.0044} | 6.08 ^{+0.34} _{-0.34} | 2.67 ^{+0.34} _{-0.34} | 0.98 | 5842 | 2.85 ^{+0.39} _{-0.39} | 30.1 | K2-195c (Mayo et al. 2018) |
| 212697709.01 | 12.193 | 3.951632 ^{+0.00030} _{-0.00030} | 3349.48035 ^{+0.0029} _{-0.0029} | 1.82 ^{+0.10} _{-0.10} | 7.40 ^{+0.61} _{-0.61} | 1.09 | 5860 | 8.77 ^{+0.73} _{-0.73} | 494 | WASP-157, K2-41 (Močnik et al. 2016) |
| 212707574.01 | 13.861 | 1.12665 ^{+0.00018} _{-0.00018} | 3346.9600 ^{+0.0047} _{-0.0047} | 2.36 ^{+0.46} _{-0.28} | 2.38 ^{+0.22} _{-0.22} | 1.63 | 5967 | 4.24 ^{+0.48} _{-0.48} | 5618 | — |
| 212735333.01 | 11.977 | 8.35812 ^{+0.00039} _{-0.00039} | 3354.6901 ^{+0.0019} _{-0.0019} | 3.30 ^{+0.16} _{-0.13} | 2.63 ^{+0.13} _{-0.13} | 0.93 | 5642 | 2.66 ^{+0.14} _{-0.12} | 121.8 | K2-197b (Mayo et al. 2018) |
| 212748535.01 | 13.582 | 5.47826 ^{+0.00034} _{-0.00034} | 3349.3152 ^{+0.0021} _{-0.0021} | 1.53 ^{+0.15} _{-0.15} | 3.51 ^{+0.33} _{-0.29} | 0.60 | 3971 | 2.30 ^{+0.23} _{-0.20} | 30.2 | — |
| 212768333.01 | 16.825 | 17.04518 ^{+0.00098} _{-0.00098} | 3360.0516 ^{+0.0018} _{-0.0018} | 3.65 ^{+0.25} _{-0.25} | 4.24 ^{+0.64} _{-0.64} | 0.77 | 5232 | 3.56 ^{+0.54} _{-0.54} | 27.2 | K2-198b (Mayo et al. 2018) |
| 212768333.02 | 16.825 | 7.44957 ^{+0.00075} _{-0.00075} | 3349.0808 ^{+0.0034} _{-0.0034} | 2.86 ^{+0.22} _{-0.22} | 2.80 ^{+0.24} _{-0.24} | 0.77 | 5232 | 2.34 ^{+0.25} _{-0.25} | 81.9 | Candidate from Pope et al. (2016) |
| 212771557.01 | 13.950 | 8.4902 ^{+0.0014} _{-0.0014} | 3349.4717 ^{+0.0047} _{-0.0047} | 2.55 ^{+0.32} _{-0.32} | 2.50 ^{+0.26} _{-0.26} | 0.86 | 5530 | 2.39 ^{+0.22} _{-0.22} | 99 | — |
| 212779563.01 | 9.945 | 6.00123 ^{+0.00012} _{-0.00012} | 3352.36041 ^{+0.00101} _{-0.00101} | 1.272 ^{+0.102} _{-0.031} | 2.75 ^{+0.11} _{-0.11} | 0.69 | 4688 | 2.064 ^{+0.088} _{-0.097} | 62.5 | Wolf 503 (Peterson et al., in prep.) |
| 212779596.01 | 11.930 | 7.37416 ^{+0.00023} _{-0.00023} | 3348.6147 ^{+0.0011} _{-0.0011} | 2.361 ^{+0.128} _{-0.091} | 4.02 ^{+0.25} _{-0.19} | 0.67 | 4772 | 2.93 ^{+0.18} _{-0.14} | 48.2 | K2-199b (Mayo et al. 2018) |
| 212779596.02 | 11.930 | 3.22575 ^{+0.00014} _{-0.00014} | 3346.9032 ^{+0.0017} _{-0.0017} | 1.872 ^{+0.151} _{-0.085} | 2.58 ^{+0.16} _{-0.16} | 0.67 | 4772 | 1.88 ^{+0.12} _{-0.12} | 145 | K2-199c (Mayo et al. 2018) |
| 212803289.01 | 11.014 | 18.24605 ^{+0.00083} _{-0.00083} | 3349.7141 ^{+0.0016} _{-0.0016} | 10.905 ^{+0.076} _{-0.085} | 3.758 ^{+0.047} _{-0.075} | 2.59 | 6560 | 10.57 ^{+0.35} _{-0.38} | 422 | K2-99b (Smith et al. 2017) |
| 212813907.01 | 14.070 | 6.72526 ^{+0.00031} _{-0.00031} | 3350.5430 ^{+0.0016} _{-0.0016} | 0.82 ^{+0.17} _{-0.13} | 5.56 ^{+1.27} _{-0.59} | 0.79 | 5007 | 4.79 ^{+1.0} _{-0.52} | 82.1 | — |
| 212870185.01 | 13.149 | 6.11665 ^{+0.00044} _{-0.00044} | 3347.9964 ^{+0.0027} _{-0.0027} | 2.54 ^{+0.28} _{-0.18} | 3.04 ^{+0.28} _{-0.25} | 1.12 | 5587 | 3.73 ^{+0.36} _{-0.32} | 258 | — |
| 251554286.01 | 12.091 | 15.46659 ^{+0.00066} _{-0.00066} | 3356.8506 ^{+0.0011} _{-0.0011} | 3.55 ^{+0.37} _{-0.42} | 4.44 ^{+0.50} _{-0.80} | 0.98 | 5657 | 4.73 ^{+0.56} _{-0.85} | 60.0 | — |
| 251582120.01 | 15.175 | 0.509967 ^{+0.00055} _{-0.00055} | 3346.9256 ^{+0.0029} _{-0.0029} | 3.25 ^{+0.36} _{-0.36} | 4.72 ^{+0.81} _{-0.74} | 1.25 | 5997 | 6.49 ^{+1.18} _{-3.9} | 10946 | — |
| 251590700.01 | 13.302 | 5.82105 ^{+0.00100} _{-0.00100} | 3347.5528 ^{+0.0053} _{-0.0053} | 6.1 ^{+0.59} _{-6.1} | 6.40 ^{+0.74} _{-0.50} | 0.86 | 5247 | 6.1 ^{+3.9} _{-3.8} | 138 | Low ρ _* , circ. |

TABLE 3
STELLAR PARAMETERS

| EPIC | Kp [mag] | BJD _{UTC} ^c [days] | S/N ^d | TRES | | | HIRES ^a | | | SpeX ^b | | | | | | | |
|------------------------|---------------|---|------------------|-------------------------|-------------------|----------------|---------------------------------------|---------------------------------------|-------------------------|-------------------|-----------------|-------------------------------------|-----|-------------------------|-------------------|---|---|
| | | | | T_{eff} [K] | $\log g$ [dex] | [M/H] [dex] | $v \sin i^e$ [km s ⁻¹] | RV ^f km s ⁻¹ | T_{eff} [K] | $\log g$ [dex] | [Fe/H] [dex] | $v \sin i$ [km s ⁻¹] | SpT | T_{eff} [K] | $\log g$ [dex] | | |
| 212428509 | 12.5 | — | — | — | — | — | — | — | — | — | — | — | — | — | — | — | — |
| 212435047 | 12.4 | — | — | — | — | — | — | — | — | — | — | — | — | — | — | — | — |
| 212460519 | 12.4 | — | — | — | — | — | — | — | — | — | — | — | — | — | — | — | — |
| 212496592 | 13.0 | 2457435.973127 | 25.4 | 5177 | 4.57 | 0.31 | 2.8 | -9.060 | — | — | — | — | — | — | — | — | — |
| 212521166 | 11.6 | 2457436.932008 | 27.7 | 4912 | 4.57 | -0.29 | 1.7 | -21.573 | — | — | — | — | — | — | — | — | — |
| 212554013 | 14.7 | — | — | — | — | — | — | — | — | — | — | — | — | — | — | — | — |
| 212572439 | 12.8 | 2457442.944484 | 16.4 | 5123 | 4.57 | 0.45 | 6.3 | 13.835 | — | — | — | — | — | — | — | — | — |
| 212580872 | 13.0 | 2457493.742254 | 30.5 | 5612 | 4.45 | 0.20 | 3.5 | -16.946 | — | — | — | — | — | — | — | — | — |
| 212586030 | 11.7 | — | — | — | — | — | — | — | — | — | — | — | — | — | — | — | — |
| 212587672 | 12.2 | — | — | — | — | — | — | — | — | — | — | — | — | — | — | — | — |
| 212619190 | 12.8 | 2458273.731631 | 28.7 | 5648 | 4.33 | 0.04 | 4.6 | 29.555 | — | — | — | — | — | — | — | — | — |
| 212628254 | 9.7 | 2458261.733258 | 51.6 | 5833 | 4.40 | -0.01 | 3.0 | -28.074 | — | — | — | — | — | — | — | — | — |
| 212628477 ⁱ | 12.5 | 2458274.706803 | 27.5 | — | — | — | — | — | — | — | — | — | — | — | — | — | — |
| 212634172 | 14.8 | — | — | — | — | — | — | — | — | — | — | — | — | — | — | — | — |
| 212651213 ⁱ | 10.8 | 2457439.912117 | 52.2 | — | — | — | — | — | — | — | — | — | — | — | — | — | — |
| " | " | 2457448.969440 | 41.0 | — | — | — | — | — | — | — | — | — | — | — | — | — | — |
| " | " | 2457449.945082 | 38.5 | — | — | — | — | — | — | — | — | — | — | — | — | — | — |
| " | " | 2457450.917452 | 37.7 | — | — | — | — | — | — | — | — | — | — | — | — | — | — |
| " | " | 2457451.909447 | 37.3 | — | — | — | — | — | — | — | — | — | — | — | — | — | — |
| " | " | 2457452.902042 | 25.8 | — | — | — | — | — | — | — | — | — | — | — | — | — | — |
| " | " | 2457454.892102 | 36.6 | — | — | — | — | — | — | — | — | — | — | — | — | — | — |
| " | " | 2457470.863085 | 37.6 | — | — | — | — | — | — | — | — | — | — | — | — | — | — |
| 212651234 ^g | 11.1 | 2457439.929578 | 49.3 | 4902 | 3.50 | 0.23 | 2.6 | -15.508 | — | — | — | — | — | — | — | — | — |
| " | " | 2457448.983742 | 27.1 | 4853 | 3.34 | 0.24 | 2.9 | -15.376 | — | — | — | — | — | — | — | — | — |
| " | " | 2457452.911059 | 15.1 | 4901 | 3.46 | 0.39 | 4.9 | -15.350 | — | — | — | — | — | — | — | — | — |
| " | " | 2457466.925434 | 32.5 | 5078 | 3.94 | 0.35 | 2.0 | -15.399 | — | — | — | — | — | — | — | — | — |
| " | " | 2457504.855779 | 23.4 | 4807 | 3.22 | 0.26 | 3.9 | -15.421 | — | — | — | — | — | — | — | — | — |
| " | " | 2457511.879130 | 20.4 | 4861 | 3.42 | 0.30 | 3.9 | -15.631 | — | — | — | — | — | — | — | — | — |
| 212686205 | 12.3 | 2457435.907480 | 28.2 | 4635 | 4.70 | -0.23 | 2.3 | -12.053 | — | — | — | — | — | — | — | — | — |
| 212689874 | 12.3 | 2457434.882603 | 29.2 | 5714 | 4.55 | -0.09 | 3.0 | -14.721 | — | — | — | — | — | — | — | — | — |
| 212697709 | 12.2 | 2457439.975173 | 40.1 | 5785 | 4.45 | 0.31 | 3.1 | -21.995 | — | — | — | — | — | — | — | — | — |
| " | " | 2457439.997975 | 39.6 | 5733 | 4.38 | 0.31 | 3.6 | -22.019 | — | — | — | — | — | — | — | — | — |
| " | " | 2457475.857401 | 34.1 | 5796 | 4.46 | 0.32 | 3.4 | -21.918 | — | — | — | — | — | — | — | — | — |
| 212705192 ⁱ | 11.7 | 2457439.893014 | 53.7 | — | — | — | — | — | — | — | — | — | — | — | — | — | — |
| 212735333 | 12.0 | 2457439.870513 | 44.5 | 5671 | 4.57 | -0.01 | 2.3 | -6.591 | — | — | — | — | — | — | — | — | — |
| 212768333 | 11.0 | 2457439.037432 | 54.1 | 5247 | 4.61 | -0.16 | 5.2 | 2.071 | — | — | — | — | — | — | — | — | — |
| 212779596 | 11.9 | 2457437.046415 | 25.6 | 4652 | 4.63 | -0.21 | 2.1 | 0.092 | — | — | — | — | — | — | — | — | — |
| 212782836 | 11.6 | — | — | — | — | — | — | — | — | — | — | — | — | — | — | — | — |
| 212779563 | 9.8 | 2458261.725801 | 45.3 | 4640 | 4.68 | -0.47 | 0.8 | -46.629 | — | — | — | — | — | — | — | — | — |
| 212803289 | 11.0 | 2457437.035094 | 42.0 | 6048 | 3.79 | 0.11 | 11.1 | -2.778 | — | — | — | — | — | — | — | — | — |
| " | " | 2457447.858765 | 37.7 | 5906 | 3.58 | 0.03 | 11.5 | -2.559 | — | — | — | — | — | — | — | — | — |
| " | " | 2457475.842684 | 29.0 | 6105 | 3.87 | 0.30 | 12.0 | -2.554 | — | — | — | — | — | — | — | — | — |
| 251539584 ⁱ | 10.8 | 2458274.726575 | 29.1 | — | — | — | — | — | — | — | — | — | — | — | — | — | — |
| " | " | 2458276.738180 | 31.3 | — | — | — | — | — | — | — | — | — | — | — | — | — | — |
| 251539609 ⁱ | 11.0 | 2458275.698478 | 35.3 | — | — | — | — | — | — | — | — | — | — | — | — | — | — |
| " | " | 2458276.730773 | 30.1 | — | — | — | — | — | — | — | — | — | — | — | — | — | — |
| 251554286 | 12.1 | 2458275.686467 | 30.5 | 5548 | 4.44 | -0.10 | 1.0 | 4.560 | — | — | — | — | — | — | — | — | — |

^a HIRES data and analysis described by (Petigura et al. 2018).

^b SpeX data and analysis described by (Dressing et al. 2017a).

^c Date of TRES observation.

^d Signal-to-noise ratio per resolution element in the wavelength range 5060 to 5315 Å.

^e SPC measures the broadening from an edge-on rotator with a fixed macroturbulent velocity of 1 km s⁻¹. Different values of macroturbulence may bias this value for slow rotators. As such, we caution against interpreting this value as $v \sin i$ without further analysis.

^f The RVs reported here have been shifted onto the IAU scale using standard star velocities, on which, e.g., HD 182488 has an absolute RV of -21.508 (Nidever et al. 2002). The uncertainties of the reconnaissance RVs on the TRES native system are typically on the order of 50 m s⁻¹ (also affected by T_{eff} , S/N and $v \sin i$), though the offset to the

TABLE 4
 ECLIPSING BINARIES

| EPIC | Kp [mag] | Epoch [BJD _{TDB}] | P [d] | T_{14} [d] | $(R_P/R_*)^2$ | comments |
|-----------|---------------|--------------------------------|------------|-----------------|---------------|--|
| 212628098 | 13.259 | 2458180.89299 | 4.352574 | 0.067307 | 0.042013 | — |
| 212651213 | 10.796 | 2458180.35821 | 2.538338 | 0.144896 | 0.044374 | V-shaped, large radius |
| 212658818 | 12.070 | 2458180.48591 | 2.321117 | 0.066364 | 0.000868 | blend because transit depth not consistent (not on target) |
| 212757601 | 16.825 | 2458179.98367 | 1.017967 | 0.057751 | 0.012362 | Jovian planet around small star? $7.7 R_{\oplus}$ |
| 212769367 | 17.911 | 2458199.34193 | 20.225392 | 0.258937 | 0.021858 | — |
| 212769682 | 18.382 | 2458199.34810 | 20.230002 | 0.276014 | 0.041586 | GAIA parallax <1 mas |
| 212871068 | 18.318 | 2458182.72856 | 8.744013 | 0.183117 | 0.140517 | — |
| 212884586 | 17.700 | 2458180.15931 | 2.882978 | 0.049651 | 0.011687 | — |
| 251810686 | 10.865 | 2458180.36230 | 2.537920 | 0.164611 | 0.059434 | bad aperture; Rappaport et al. (2016) |
| 212581374 | 10.292 | 2458180.14795 | 0.784498 | 0.157174 | 0.003875 | — |
| 212406350 | 13.923 | 2458179.72331 | 0.833679 | 0.083508 | 0.096367 | — |
| 212409856 | 13.446 | 2458179.83675 | 0.531704 | 0.078146 | 0.159770 | — |
| 212417656 | 12.745 | 2458179.74444 | 0.815627 | 0.136918 | 0.023504 | — |
| 212420474 | 13.442 | 2458179.83016 | 0.600579 | 0.066488 | 0.044711 | — |
| 212420510 | 14.632 | 2458179.82589 | 0.600656 | 0.077941 | 0.145720 | contact |
| 212421319 | 16.407 | 2458182.18746 | 5.528665 | 0.239914 | 0.014466 | odd-even, wrong period |
| 212421673 | 13.172 | 2458187.99492 | 28.248155 | 0.446599 | 0.003888 | — |
| 212426112 | 13.150 | 2458179.89122 | 1.530195 | 0.072284 | 0.035180 | — |
| 212428509 | 12.483 | 2458180.30248 | 2.667940 | 0.080248 | 0.007745 | odd-even effect |
| 212435964 | 14.080 | 2458193.11111 | 25.184817 | 0.201155 | 0.234665 | — |
| 212439709 | 14.352 | 2458180.15803 | 1.218136 | 0.066728 | 0.056980 | contact, same as 1 |
| 212442107 | 15.821 | 2458180.02735 | 0.546059 | 0.074620 | 0.273964 | — |
| 212442408 | 11.778 | 2458180.41810 | 0.909676 | 0.123028 | 0.255280 | — |
| 212453473 | 13.957 | 2458181.97486 | 2.756129 | 0.150371 | 0.323040 | — |
| 212454161 | 15.225 | 2458180.76138 | 22.334245 | 0.610513 | 0.022610 | — |
| 212455982 | 14.140 | 2458180.67276 | 1.620017 | 0.242113 | 0.107147 | — |
| 212456583 | 13.429 | 2458182.17512 | 2.877393 | 0.164731 | 0.161885 | — |
| 212460623 | 9.086 | 2458179.98967 | 0.492488 | 0.086255 | 0.000156 | — |
| 212465919 | 15.159 | 2458180.05317 | 0.569619 | 0.081742 | 0.230555 | contacting |
| 212468149 | 14.814 | 2458179.86667 | 0.688366 | 0.059358 | 0.114282 | — |
| 212473154 | 8.980 | 2458181.23537 | 1.816975 | 0.083992 | 0.002040 | — |
| 212481328 | 13.090 | 2458179.55397 | 3.417361 | 0.105410 | 0.048337 | — |
| 212488008 | 10.633 | 2458189.49044 | 11.334688 | 0.070855 | 0.001533 | — |
| 212491978 | 14.025 | 2458179.95415 | 0.535811 | 0.062105 | 0.071267 | contact ,same as 1 |
| 212497267 | 12.282 | 2458182.01007 | 3.744355 | 0.180382 | 0.285638 | — |
| 212499716 | 13.748 | 2458180.06238 | 0.874745 | 0.035389 | 0.001790 | — |
| 212502064 | 9.671 | 2458179.70262 | 0.560679 | 0.088106 | 0.049133 | contact |
| 212504385 | 13.842 | 2458179.91896 | 0.826894 | 0.122608 | 0.249751 | — |
| 212509737 | 11.997 | 2458179.59591 | 2.343356 | 0.059597 | 0.008323 | — |
| 212511920 | 13.209 | 2458179.99753 | 0.572508 | 0.076707 | 0.097044 | contact |
| 212512022 | 16.643 | 2458179.89864 | 0.514313 | 0.124243 | 0.002423 | contact |
| 212518838 | 15.643 | 2458179.80762 | 0.651904 | 0.081742 | 0.198824 | contact |
| 212523277 | 17.547 | 2458179.75820 | 13.538932 | 0.114329 | 0.087378 | — |
| 212527975 | 13.708 | 2458179.68204 | 0.517780 | 0.081742 | 0.157632 | contact |
| 212530520 | 15.411 | 2458180.29465 | 0.808487 | 0.093941 | 0.118684 | contact |
| 212535959 | 13.803 | 2458190.36673 | 17.733194 | 0.292331 | 0.111249 | — |
| 212537106 | 12.982 | 2458181.36656 | 9.263450 | 0.273879 | 0.163254 | — |
| 212540174 | 14.869 | 2458179.57468 | 0.527054 | 0.040555 | 0.056895 | contact |
| 212540985 | 13.574 | 2458179.85092 | 0.548227 | 0.078714 | 0.035505 | — |
| 212541386 | 14.231 | 2458181.74987 | 3.630331 | 0.091115 | 0.074444 | — |
| 212545451 | 15.672 | 2458179.79113 | 1.133767 | 0.154570 | 0.450641 | — |
| 212545602 | 16.209 | 2458180.61219 | 1.756713 | 0.220238 | 0.670509 | — |
| 212546446 | 14.369 | 2458179.68614 | 0.655294 | 0.081742 | 0.133002 | contact |
| 212553193 | 15.314 | 2458179.68060 | 0.570422 | 0.079264 | 0.233006 | — |
| 212559866 | 11.864 | 2458184.00383 | 19.702223 | 0.383548 | 0.248986 | — |
| 212560752 | 12.839 | 2458179.91313 | 0.582783 | 0.081742 | 0.097117 | — |
| 212566769 | 13.331 | 2458189.13230 | 14.301229 | 0.323096 | 0.039127 | — |
| 212567829 | 18.076 | 2458180.10226 | 0.841796 | 0.119074 | 0.284914 | — |
| 212570257 | 12.523 | 2458179.69542 | 0.610230 | 0.055085 | 0.070548 | secondary of contacting |
| 212577519 | 14.234 | 2458180.54062 | 0.980712 | 0.077982 | 0.115798 | contact |
| 212579164 | 13.632 | 2458182.64844 | 18.155715 | 0.137503 | 0.230781 | $46 R_{\oplus}$ |
| 212580081 | 18.233 | 2458180.41422 | 1.491851 | 0.088955 | 0.692969 | $35 R_{\oplus}$ |
| 212580230 | 12.838 | 2458179.96998 | 0.563909 | 0.081742 | 0.367660 | Contact |
| 212586717 | 13.875 | 2458181.71797 | 4.295939 | 0.087219 | 0.012705 | — |
| 212601505 | 14.486 | 2458179.96618 | 0.724453 | 0.035719 | 0.020973 | — |
| 212609851 | 15.164 | 2458179.82750 | 0.642765 | 0.057191 | 0.223025 | — |
| 212611243 | 14.163 | 2458179.94634 | 0.726623 | 0.077036 | 0.097420 | — |
| 212612033 | 18.300 | 2458179.98494 | 1.049595 | 0.091376 | 0.022397 | — |
| 212613128 | 13.861 | 2458180.19045 | 0.759210 | 0.070657 | 0.213789 | — |
| 212615099 | 15.660 | 2458192.20124 | 16.397313 | 0.105083 | 0.122559 | — |
| 212617879 | 12.316 | 2458179.84646 | 2.210766 | 0.153759 | 0.142075 | — |
| 212627712 | 13.265 | 2458186.21980 | 19.913432 | 0.145782 | 0.165860 | $107 R_{\oplus}$ |
| 212629807 | 15.143 | 2458179.90970 | 0.501935 | 0.081742 | 0.206343 | contact |

TABLE 4 — *Continued*

| EPIC | K_p [mag] | Epoch [BJD _{TDB}] | P [d] | T_{14} [d] | $(R_P/R_*)^2$ | comments |
|-----------|----------------|--------------------------------|------------|-----------------|---------------|--|
| 212631911 | 15.546 | 2458179.98736 | 0.520852 | 0.078445 | 0.333555 | — |
| 212634594 | 15.202 | 2458184.28069 | 6.401944 | 0.145015 | 0.212873 | — |
| 212641218 | 14.993 | 2458179.98311 | 1.049606 | 0.076901 | 0.001691 | — |
| 212644753 | 9.422 | 2458179.97694 | 1.049846 | 0.097062 | 0.041131 | — |
| 212651213 | 10.796 | 2458191.53766 | 13.196894 | 0.199239 | 0.010896 | Rappaport et al. (2016) |
| 212651234 | 11.139 | 2458180.35324 | 2.538731 | 0.123252 | 0.008702 | Rappaport et al. (2016); 30.5 R_{\oplus} |
| 212652663 | 14.819 | 2458180.77106 | 1.669747 | 0.102005 | 0.228074 | — |
| 212654750 | 13.917 | 2458179.88743 | 0.529294 | 0.081742 | 0.413695 | contact |
| 212657659 | 17.470 | 2458180.01607 | 0.546679 | 0.055120 | 0.014074 | contact |
| 212666524 | 14.293 | 2458179.90638 | 0.670516 | 0.081742 | 0.121268 | — |
| 212666639 | 15.366 | 2458179.54065 | 0.541019 | 0.079310 | 0.301795 | contact |
| 212667298 | 12.902 | 2458179.54657 | 0.606965 | 0.081742 | 0.435121 | contact |
| 212671857 | 13.697 | 2458180.24217 | 0.727391 | 0.068894 | 0.139981 | — |
| 212679798 | 14.846 | 2458180.12895 | 1.834750 | 0.073377 | 0.033351 | — |
| 212686943 | 13.774 | 2458181.02088 | 1.578709 | 0.165925 | 0.064449 | — |
| 212687040 | 13.475 | 2458180.27371 | 1.852983 | 0.106111 | 0.205153 | — |
| 212689699 | 17.593 | 2458180.07219 | 0.518523 | 0.130845 | 0.013282 | contact |
| 212690087 | 14.746 | 2458180.09903 | 0.786832 | 0.114912 | 0.042193 | — |
| 212691727 | 12.657 | 2458184.17922 | 12.862016 | 0.201678 | 0.050839 | — |
| 212695400 | 15.403 | 2458180.22806 | 0.848459 | 0.065686 | 0.215148 | — |
| 212697951 | 12.582 | 2458180.27911 | 1.912398 | 0.114449 | 0.259949 | star spot causes modulation |
| 212701118 | 12.691 | 2458179.72465 | 2.434027 | 0.144225 | 0.661748 | — |
| 212702889 | 14.558 | 2458179.93264 | 0.631071 | 0.056983 | 0.052287 | — |
| 212705192 | 11.728 | 2458181.41157 | 2.268360 | 0.048411 | 0.005948 | odd-even effect, double-lined |
| 212705508 | 14.415 | 2458180.05063 | 0.603816 | 0.044304 | 0.003131 | — |
| 212707624 | 13.179 | 2458182.00981 | 3.604588 | 0.207304 | 0.106715 | — |
| 212708296 | 15.906 | 2458180.26857 | 0.803247 | 0.100811 | 0.466097 | — |
| 212708783 | 10.386 | 2458179.95230 | 2.253755 | 0.142294 | 0.118586 | — |
| 212710571 | 17.458 | 2458179.95368 | 2.253558 | 0.104992 | 0.012538 | — |
| 212712870 | 15.304 | 2458179.96661 | 0.494226 | 0.069594 | 0.249001 | — |
| 212716448 | 18.478 | 2458180.01069 | 0.546752 | 0.058736 | 0.062706 | same as 1 |
| 212723069 | 14.817 | 2458186.05758 | 11.495130 | 0.232389 | 0.037574 | — |
| 212723581 | 15.961 | 2458180.00972 | 0.600845 | 0.066764 | 0.124436 | same signal as 1 |
| 212733831 | 14.786 | 2458179.70777 | 0.732994 | 0.081742 | 0.117807 | — |
| 212734205 | 17.588 | 2458181.12287 | 4.965604 | 0.493681 | 0.397380 | — |
| 212737890 | 15.875 | 2458179.84702 | 0.880552 | 0.105444 | 0.127097 | — |
| 212740148 | 13.996 | 2458180.15919 | 0.741042 | 0.030996 | 0.011375 | — |
| 212741343 | 15.933 | 2458180.05956 | 0.580501 | 0.054682 | 0.100483 | contact |
| 212746282 | 12.518 | 2458179.85030 | 0.595119 | 0.081742 | 0.093743 | contact |
| 212747879 | 15.717 | 2458179.97540 | 0.705760 | 0.081742 | 0.331363 | — |
| 212748031 | 15.678 | 2458180.36357 | 0.887395 | 0.037098 | 0.005056 | — |
| 212751079 | 13.700 | 2458179.62410 | 0.595131 | 0.142401 | 0.264229 | — |
| 212751916 | 13.890 | 2458180.64439 | 15.715606 | 0.097758 | 0.004367 | — |
| 212759326 | 13.892 | 2458182.52706 | 3.376283 | 0.117698 | 0.076310 | — |
| 212770429 | 11.153 | 2458199.35119 | 20.225506 | 0.342386 | 0.210533 | 75 R_{\oplus} |
| 212771092 | 17.554 | 2458180.04000 | 0.613816 | 0.081742 | 0.513770 | — |
| 212771522 | 14.105 | 2458180.36577 | 0.964855 | 0.036899 | 0.002141 | — |
| 212773272 | 14.965 | 2458182.45629 | 4.681890 | 0.080497 | 0.043560 | — |
| 212773309 | 11.391 | 2458182.45642 | 4.681764 | 0.093543 | 0.074791 | — |
| 212781530 | 15.601 | 2458180.03084 | 0.574416 | 0.081742 | 0.518721 | contact |
| 212781903 | 13.952 | 2458179.93093 | 0.516312 | 0.081742 | 0.057071 | — |
| 212786474 | 14.472 | 2458179.57656 | 9.271273 | 0.151254 | 0.429256 | — |
| 212789681 | 13.740 | 2458179.55289 | 0.497467 | 0.116872 | 0.000516 | contact |
| 212796590 | 16.506 | 2458179.97098 | 0.555792 | 0.144363 | 0.009497 | contact |
| 212801119 | 12.771 | 2458180.11071 | 0.591442 | 0.045596 | 0.019034 | — |
| 212801667 | 11.911 | 2458186.41163 | 23.274142 | 0.214440 | 0.075892 | — |
| 212805198 | 14.422 | 2458180.96489 | 3.228788 | 0.086784 | 0.079089 | — |
| 212812349 | 13.712 | 2458185.62953 | 8.167374 | 0.174965 | 0.069996 | — |
| 212814517 | 15.896 | 2458179.76158 | 0.624914 | 0.079529 | 0.314121 | — |
| 212822491 | 11.078 | 2458186.08017 | 14.321271 | 0.265478 | 0.171877 | — |
| 212824416 | 16.638 | 2458179.85284 | 0.590807 | 0.057018 | 0.134113 | contact EB; secondary |
| 212826509 | 16.297 | 2458180.41915 | 0.988762 | 0.113296 | 0.311666 | — |
| 212827749 | 13.358 | 2458185.76643 | 11.345548 | 0.187133 | 0.207902 | — |
| 212828964 | 16.170 | 2458179.90943 | 0.646399 | 0.142256 | 0.001916 | contact |
| 212834326 | 15.554 | 2458180.10438 | 0.780977 | 0.079370 | 0.242254 | — |
| 212837770 | 16.663 | 2458180.22595 | 0.850575 | 0.064098 | 0.263615 | — |
| 212839815 | 12.874 | 2458180.59961 | 4.441165 | 0.198630 | 0.037661 | — |
| 212842049 | 16.894 | 2458181.48623 | 3.289052 | 0.066265 | 0.062749 | — |
| 212842366 | 12.081 | 2458179.58419 | 0.543994 | 0.059710 | 0.018823 | — |
| 212854191 | 12.566 | 2458180.39309 | 0.868807 | 0.099834 | 0.046954 | contact |
| 212864075 | 11.826 | 2458180.11467 | 0.729410 | 0.071462 | 0.015258 | — |
| 212866286 | 12.702 | 2458180.51003 | 4.717350 | 0.245227 | 0.178060 | — |
| 212869892 | 12.392 | 2458179.99254 | 0.814852 | 0.057258 | 0.008050 | — |
| 212872008 | 14.464 | 2458180.76477 | 1.311925 | 0.107024 | 0.102602 | — |

TABLE 4 — *Continued*

| EPIC | K_p [mag] | Epoch [BJD _{TDB}] | P [d] | T_{14} [d] | $(R_p/R_*)^2$ | comments |
|-----------|----------------|--------------------------------|------------|-----------------|---------------|---|
| 212872519 | 18.895 | 2458180.02866 | 1.361929 | 0.188677 | 0.316683 | — |
| 212878430 | 18.479 | 2458179.64683 | 0.511345 | 0.081742 | 0.086995 | contact |
| 212884295 | 16.098 | 2458180.05753 | 0.632894 | 0.082281 | 0.151918 | contact |
| 212885442 | 15.582 | 2458179.58563 | 0.626888 | 0.081742 | 0.192118 | — |
| 251505087 | 16.021 | 2458180.01374 | 0.744603 | 0.080170 | 0.204046 | — |
| 251505480 | 18.300 | 2458179.54528 | 0.622504 | 0.080448 | 0.117676 | contact |
| 251505499 | 9.619 | 2458179.54539 | 0.622507 | 0.081742 | 0.278995 | contact |
| 251508456 | 15.216 | 2458179.90526 | 0.774116 | 0.142628 | 0.773576 | — |
| 251508975 | 16.979 | 2458179.93148 | 0.583320 | 0.081742 | 0.142980 | — |
| 251512942 | 14.262 | 2458179.54192 | 0.546855 | 0.081742 | 0.249001 | contacting |
| 251523672 | 16.201 | 2458179.84407 | 0.594784 | 0.043602 | 0.153440 | contact |
| 251524025 | 16.805 | 2458179.79873 | 0.638134 | 0.073617 | 0.386702 | — |
| 251539042 | 15.597 | 2458179.53378 | 0.561767 | 0.076747 | 0.249001 | — |
| 251543556 | 13.596 | 2458179.96760 | 0.498006 | 0.049089 | 0.018157 | — |
| 251551459 | 16.526 | 2458179.76260 | 0.938771 | 0.083508 | 0.235088 | — |
| 251566115 | 12.519 | 2458182.48929 | 11.850868 | 0.127530 | 0.072908 | — |
| 251567015 | 16.442 | 2458179.68328 | 0.558434 | 0.073032 | 0.111879 | contact |
| 251571270 | 17.339 | 2458179.61675 | 0.645707 | 0.048994 | 0.425897 | — |
| 251575183 | 18.642 | 2458179.89846 | 0.515838 | 0.070330 | 0.116968 | — |
| 251600179 | 17.983 | 2458179.74495 | 0.668258 | 0.055939 | 0.071262 | — |
| 251606815 | 15.059 | 2458179.53572 | 0.514761 | 0.081742 | 0.405411 | — |
| 251612064 | 15.053 | 2458179.72566 | 0.519174 | 0.081742 | 0.367738 | — |
| 251613109 | 17.532 | 2458180.09242 | 0.603096 | 0.075259 | 0.282421 | — |
| 251628925 | 12.632 | 2458197.00901 | 23.932888 | 0.374788 | 0.073781 | — |
| 251809768 | 18.310 | 2458182.00880 | 3.744813 | 0.132943 | 0.027276 | — |
| 251809787 | 16.978 | 2458180.14621 | 0.874333 | 0.111146 | 0.174670 | — |
| 251809799 | 18.088 | 2458179.77296 | 0.929420 | 0.101403 | 0.209458 | — |
| 251809801 | 18.209 | 2458180.14037 | 5.424922 | 0.239628 | 0.047817 | — |
| 251809804 | 18.366 | 2458181.02178 | 3.044908 | 0.394803 | 0.336826 | — |
| 251809805 | 18.431 | 2458179.87263 | 0.493215 | 0.072998 | 0.260563 | contact |
| 251809808 | 18.531 | 2458179.64709 | 0.986293 | 0.204333 | 0.341796 | — |
| 251809809 | 18.694 | 2458179.63921 | 0.543684 | 0.081742 | 0.091127 | contact |
| 251809830 | 19.404 | 2458180.01339 | 0.746323 | 0.081742 | 0.313398 | — |
| 251809968 | 19.390 | 2458179.54579 | 0.622505 | 0.081742 | 0.185758 | — |
| 251810686 | 10.865 | 2458186.24598 | 13.191424 | 0.151051 | 0.012218 | quintuple system, Rappaport et al. (2016) |
| 251539584 | 10.763 | 2458179.55118 | 1.088222 | 0.045042 | 0.000625 | SB2, blend with 251539609 |
| 251539609 | 11.016 | 2458179.55151 | 1.088213 | 0.044667 | 0.000624 | SB2, blend with 251539584 |

TABLE 5
OTHER PERIODIC VARIABLES

| EPIC | K_p [mag] | P [d] | comments |
|-----------|----------------|------------|---------------------|
| 212404864 | 17.754 | 0.583854 | — |
| 212416035 | 18.061 | 0.650274 | — |
| 212424629 | 16.018 | 0.651446 | — |
| 212424861 | 17.877 | 0.651436 | — |
| 212425817 | 16.684 | 0.715986 | RR Lyrae |
| 212426904 | 15.519 | 1.559636 | — |
| 212429810 | 9.835 | 1.751454 | — |
| 212431975 | 12.460 | 0.560643 | — |
| 212433098 | 14.338 | 0.755435 | — |
| 212433328 | 14.893 | 1.155617 | — |
| 212439709 | 14.352 | 0.609047 | contact? |
| 212440192 | 16.146 | 0.531711 | — |
| 212441076 | 14.847 | 0.528502 | — |
| 212443701 | 16.789 | 0.683153 | — |
| 212449290 | 16.309 | 0.847446 | — |
| 212449840 | 14.091 | 0.558064 | — |
| 212450261 | 12.888 | 3.746695 | — |
| 212453596 | 16.109 | 0.595544 | — |
| 212460039 | 9.020 | 0.571204 | — |
| 212461484 | 7.976 | 2.268343 | — |
| 212463213 | 14.966 | 0.644204 | — |
| 212467265 | 16.591 | 0.617039 | — |
| 212469922 | 12.509 | 0.810722 | — |
| 212470542 | 14.767 | 0.501587 | — |
| 212470959 | 16.904 | 0.909599 | — |
| 212475454 | 14.591 | 0.495057 | — |
| 212476230 | 14.065 | 0.909933 | — |
| 212476743 | 16.906 | 0.626211 | — |
| 212476895 | 12.756 | 0.806344 | — |
| 212478962 | 15.411 | 0.609325 | — |
| 212479061 | 18.334 | 0.491113 | — |
| 212481276 | 14.791 | 0.560738 | — |
| 212491978 | 14.025 | 0.535797 | — |
| 212492961 | 12.942 | 0.746502 | — |
| 212503342 | 8.324 | 0.501263 | — |
| 212504059 | 11.601 | 0.505806 | — |
| 212506921 | 16.857 | 0.537091 | — |
| 212506981 | 18.107 | 0.560708 | — |
| 212519490 | 12.859 | 0.553239 | — |
| 212520127 | 16.474 | 0.787684 | — |
| 212529254 | 15.890 | 1.224833 | — |
| 212530684 | 17.050 | 0.505286 | large OOT amplitude |
| 212534342 | 17.713 | 0.617741 | — |
| 212537690 | 16.567 | 0.605773 | — |
| 212540092 | 17.920 | 0.558487 | — |
| 212542474 | 12.033 | 0.526188 | — |
| 212551424 | 13.270 | 0.634884 | — |
| 212555590 | 14.733 | 0.636359 | — |
| 212560096 | 14.764 | 0.599002 | — |
| 212561206 | 15.129 | 0.615971 | — |
| 212562145 | 14.856 | 0.728760 | — |
| 212564937 | 14.129 | 0.506676 | — |
| 212570257 | 12.523 | 0.610247 | — |
| 212575000 | 16.145 | 0.735286 | — |
| 212575799 | 15.277 | 0.616666 | — |
| 212575959 | 12.439 | 0.670392 | — |
| 212578200 | 13.144 | 1.131015 | — |
| 212589990 | 12.178 | 0.504842 | — |
| 212594525 | 15.888 | 0.762575 | — |
| 212597328 | 18.187 | 0.658850 | RR Lyrae |
| 212601233 | 14.997 | 0.636031 | — |
| 212603282 | 12.328 | 0.696329 | — |
| 212603536 | 11.933 | 0.720349 | — |
| 212603999 | 15.443 | 0.502387 | RR Lyrae |
| 212609833 | 16.543 | 0.570110 | — |
| 212612729 | 14.534 | 0.904916 | — |
| 212617685 | 13.406 | 0.594009 | — |
| 212619206 | 15.542 | 0.687767 | — |
| 212620826 | 13.616 | 0.789620 | — |
| 212621423 | 14.951 | 0.817041 | — |
| 212628986 | 15.071 | 1.428411 | — |
| 212631286 | 13.236 | 0.525008 | — |
| 212631414 | 13.022 | 0.525005 | — |
| 212631757 | 16.082 | 0.175266 | — |

TABLE 5 — *Continued*

| EPIC | K_p [mag] | P [d] | comments |
|-----------|----------------|------------|----------|
| 212636050 | 15.543 | 0.630885 | — |
| 212639395 | 16.928 | 0.591004 | — |
| 212639932 | 16.316 | 0.619463 | — |
| 212640806 | 15.889 | 0.510041 | — |
| 212642195 | 14.144 | 0.629391 | — |
| 212644219 | 16.174 | 0.622971 | — |
| 212648945 | 13.771 | 0.750334 | — |
| 212659834 | 11.665 | 0.546711 | — |
| 212666537 | 16.115 | 0.494617 | — |
| 212669531 | 13.967 | 0.606174 | — |
| 212672666 | 16.536 | 0.520714 | — |
| 212674862 | 15.842 | 0.675189 | — |
| 212676658 | 10.640 | 0.532304 | — |
| 212699845 | 17.389 | 0.616183 | — |
| 212703179 | 11.251 | 0.673494 | — |
| 212704410 | 10.588 | 0.762124 | — |
| 212706992 | 14.171 | 0.573939 | — |
| 212711185 | 15.760 | 0.676885 | — |
| 212711671 | 14.949 | 0.545729 | — |
| 212715425 | 14.822 | 0.542155 | — |
| 212716271 | 15.192 | 0.546693 | — |
| 212716448 | 18.478 | 0.546688 | — |
| 212716631 | 18.970 | 0.573803 | — |
| 212717166 | 16.262 | 0.586327 | — |
| 212718800 | 13.631 | 0.650108 | — |
| 212719030 | 15.126 | 1.349336 | — |
| 212720186 | 16.530 | 0.626749 | — |
| 212722087 | 12.587 | 0.546000 | — |
| 212722872 | 14.345 | 0.692869 | — |
| 212723581 | 15.961 | 0.600851 | — |
| 212730754 | 17.858 | 0.587020 | — |
| 212732420 | 13.805 | 0.546859 | — |
| 212733211 | 16.553 | 0.592465 | — |
| 212735753 | 17.112 | 0.611941 | — |
| 212736684 | 18.155 | 0.548902 | — |
| 212742333 | 18.142 | 0.582756 | — |
| 212749368 | 16.551 | 0.630246 | — |
| 212755404 | 13.810 | 0.758773 | — |
| 212760038 | 11.199 | 0.598949 | — |
| 212766036 | 16.427 | 1.128395 | — |
| 212775050 | 16.256 | 0.633570 | — |
| 212775136 | 13.127 | 0.520693 | — |
| 212783579 | 13.453 | 0.623693 | — |
| 212784817 | 15.000 | 0.735008 | — |
| 212785152 | 15.295 | 0.688545 | — |
| 212791551 | 19.214 | 0.720158 | — |
| 212791701 | 16.337 | 0.533695 | — |
| 212793961 | 12.154 | 0.633511 | — |
| 212794694 | 17.778 | 0.505073 | — |
| 212794999 | 16.022 | 0.602511 | — |
| 212795516 | 17.724 | 0.613296 | — |
| 212798939 | 16.823 | 0.507892 | — |
| 212801998 | 15.450 | 0.517430 | — |
| 212808944 | 13.005 | 0.670074 | — |
| 212812050 | 13.882 | 0.575880 | — |
| 212814000 | 14.807 | 0.561011 | — |
| 212814419 | 18.297 | 0.625019 | — |
| 212814441 | 14.201 | 0.783737 | — |
| 212818222 | 16.219 | 0.584496 | — |
| 212818294 | 16.194 | 0.829784 | — |
| 212820594 | 14.665 | 0.530704 | — |
| 212821516 | 11.946 | 0.508947 | — |
| 212824416 | 16.638 | 0.590808 | — |
| 212827294 | 16.930 | 0.559323 | — |
| 212828640 | 14.934 | 0.592274 | — |
| 212828933 | 14.283 | 0.716170 | — |
| 212829102 | 12.264 | 0.500330 | — |
| 212829130 | 16.467 | 0.646563 | — |
| 212829294 | 17.079 | 0.754500 | — |
| 212830414 | 16.810 | 0.571236 | — |
| 212831062 | 15.007 | 0.705463 | — |
| 212831234 | 13.076 | 0.649151 | — |
| 212833004 | 9.158 | 0.543036 | — |
| 212835551 | 12.676 | 0.562135 | — |
| 212835780 | 16.332 | 1.673125 | — |

TABLE 5 — *Continued*

| EPIC | K_p [mag] | P [d] | comments |
|-----------|----------------|------------|----------|
| 212847938 | 15.743 | 0.607034 | — |
| 212853330 | 16.549 | 0.587536 | — |
| 212862638 | 15.191 | 0.497067 | — |
| 212867164 | 17.189 | 0.572633 | — |
| 212869088 | 17.220 | 0.505407 | — |
| 212870977 | 14.714 | 0.507252 | — |
| 212873395 | 12.808 | 0.605284 | — |
| 212879205 | 12.829 | 0.649341 | — |
| 212879653 | 11.576 | 0.517211 | — |
| 212881555 | 17.099 | 0.545534 | — |
| 212882485 | 15.839 | 0.624794 | — |
| 212882871 | 19.921 | 0.612855 | — |
| 212883764 | 15.503 | 0.668488 | — |
| 212884307 | 13.143 | 0.583500 | — |
| 229228086 | 17.360 | 0.620306 | — |
| 229228087 | 17.630 | 0.602832 | — |
| 229228091 | 18.240 | 0.600837 | — |
| 229228112 | 17.940 | 0.591997 | — |
| 229228121 | 17.770 | 0.574762 | — |
| 251501619 | 14.964 | 0.580914 | — |
| 251502557 | 13.714 | 0.679484 | — |
| 251504831 | 17.611 | 0.622515 | — |
| 251504891 | 9.777 | 0.528140 | — |
| 251505259 | 17.675 | 0.622474 | — |
| 251509348 | 16.172 | 0.623298 | — |
| 251517127 | 18.061 | 0.714932 | — |
| 251519864 | 11.446 | 1.275710 | — |
| 251520093 | 18.417 | 0.540185 | — |
| 251523672 | 16.201 | 0.594779 | — |
| 251526009 | 18.424 | 0.672721 | — |
| 251529654 | 16.234 | 0.521895 | — |
| 251530257 | 17.204 | 0.641235 | — |
| 251540409 | 16.770 | 0.537995 | — |
| 251554210 | 16.357 | 0.509245 | — |
| 251564868 | 18.244 | 0.494339 | — |
| 251566981 | 11.096 | 0.518554 | — |
| 251568443 | 14.911 | 0.714645 | — |
| 251569406 | 14.271 | 0.670480 | — |
| 251574051 | 13.248 | 2.206687 | — |
| 251578582 | 11.275 | 7.120210 | — |
| 251579007 | 14.922 | 0.629344 | — |
| 251583296 | 17.090 | 0.549769 | — |
| 251583388 | 14.011 | 0.950893 | — |
| 251585662 | 19.180 | 0.646642 | — |
| 251590688 | 12.081 | 0.710497 | — |
| 251596880 | 10.890 | 2.633147 | — |
| 251599500 | 15.101 | 0.571171 | — |
| 251602987 | 17.865 | 0.688673 | — |
| 251608983 | 12.951 | 0.934933 | — |
| 251611842 | 12.691 | 0.518191 | — |
| 251612403 | 15.626 | 0.698081 | — |
| 251613106 | 17.050 | 0.717477 | — |
| 251615995 | 14.797 | 0.561389 | — |
| 251809762 | 17.770 | 0.574708 | — |
| 251809767 | 18.290 | 0.609255 | — |
| 251809792 | 17.702 | 0.582034 | — |
| 251809793 | 17.830 | 0.535073 | — |
| 251809794 | 17.837 | 0.514385 | — |
| 251809800 | 18.158 | 0.644357 | — |
| 251809802 | 18.232 | 0.565049 | — |
| 251809803 | 18.271 | 0.538007 | — |
| 251809807 | 18.499 | 0.605395 | — |
| 251809812 | 18.954 | 0.615473 | — |
| 251809817 | 19.009 | 0.598227 | — |
| 251809820 | 19.110 | 0.573687 | — |
| 251809824 | 19.182 | 0.709409 | — |
| 251809836 | 19.611 | 0.591795 | — |
| 251809865 | 20.310 | 0.669433 | — |
| 251810875 | 18.667 | 0.643312 | — |
| 251811189 | 18.981 | 0.560705 | — |
| 251811486 | 19.100 | 0.798840 | — |
| 251811829 | 19.187 | 0.651565 | — |
| 251809821 | 19.110 | 0.610251 | — |

TABLE 5 — *Continued*

| EPIC | K_p [mag] | P [d] | comments |
|------|----------------|------------|----------|
|------|----------------|------------|----------|